Received: 29 November 2023 | Revised: 8 April 2024 | Accepted: 11 April 2024

DOI: 10.1111/ffe.14319

ORIGINAL ARTICLE

FFEMS Fatigue & Fracture of Engineering Materials & Structures WILEY

Multiaxial fatigue assessment of welded joints: A review of Eurocode 3 and International Institute of Welding criteria with different stress analysis approaches

Chin Tze Ng[1] | **Cetin Morris Sonsino**[2] | **Luca Susmel**[1]

[1]Department of Civil and Structural Engineering, The University of Sheffield, Sheffield, UK

[2]Fraunhofer Institute for Structural Durability and System Reliability LBF, Darmstadt, Germany

Correspondence
Luca Susmel, Department of Civil and Structural Engineering, The University of Sheffield, Mappin Street, Sheffield, S1 3JD, UK.
Email: l.susmel@sheffield.ac.uk

Abstract

This paper reviews quantitively the multiaxial fatigue assessment of steel and aluminum welded joints, focusing on Eurocodes (ECs) and the recommendations of the International Institute of Welding (IIW). Extensive fatigue data under constant and variable amplitude loading are reanalyzed using stress analysis approaches such as nominal stress, hot spot stress, and effective notch stress. Evaluation of the ECs and IIW criteria reveals an effective assessment of multiaxial fatigue, with a satisfactory level of conservatism. Further research is needed especially for variable amplitude (VA) loading to enhance the precision and reliability of assessments, contributing to improved design practices and structural integrity in welded joint applications.

KEYWORDS

constant amplitude, effective notch stress, Eurocode 3 (EC3), hot spot stress, International Institute of Welding (IIW), multiaxial fatigue, nominal stress, variable amplitude, welded joints

Highlights

1. The multiaxial fatigue criteria proposed by EC3 and the IIW are reviewed
2. Design criteria are applied in terms of nominal, hot spot, and effective notch stress
3. Both constant and variable amplitude load histories are considered
4. Standard approaches are characterized by a large level of conservatism

1 | INTRODUCTION

The significance of welding technology spans across various industries, such as bridge construction, automotive manufacturing, and offshore structures, offering a multitude of advantages, particularly in structural applications. However, the susceptibility of welded joints to fatigue failure presents a major challenge. This problem becomes further intricate when considering the presence of multiaxial fatigue loading.

TABLE 1 Summary of allowable damage sums under CA and VA fatigue loading for various loading scenarios and materials.

		Allowable damage sum (CA)		Allowable damage sum/comparison value (VA)		
Material	**Normal and shear stress**	D_{IIW}	D_{IIW}	D_{IIW}	CV_{IIW}	D_{IIW}
Steel	Proportional	1.0	1.0	1.0	1.0	0.5
	Non-proportional	1.0	0.5	1.0	0.5	0.5
Aluminum	Proportional	1.0	1.0	1.0	1.0	0.5
	Non-proportional	1.0	1.0	1.0	1.0	0.5

To fully harness the potential of welding and ensure optimal structural integrity under multiaxial fatigue conditions, adherence to relevant standard codes and guidelines is paramount. Eurocodes (ECs) and the recommendations from the International Institute of Welding (IIW) provide essential direction and criteria for assessing the fatigue performance of welded joints.[1–3]

Concurrently, it is crucial for engineers to possess a comprehensive understanding of the underlying principles governing the multiaxial fatigue assessment criteria proposed by these standards. By recognizing both the strengths and limitations of these criteria, engineers can apply them judiciously in diverse scenarios, ensuring accurate and reliable assessments.

This paper specifically focuses on welded joints using two commonly employed structural materials: aluminum and steel. Its primary objective is to comprehensively review and assess the reliability, accuracy, level of conservatism, and robustness of those multiaxial fatigue assessment criteria proposed by ECs and the IIW. The investigation commences by establishing a strong foundational understanding through reanalysis of welded joints subjected to constant amplitude (CA) multiaxial fatigue loading. Subsequently, the investigation extends to reanalyzing welded joints under variable amplitude (VA) multiaxial fatigue loading, offering a more accurate reflection of real-life scenarios. This meticulous approach facilitates a thorough exploration of the criteria and their practical implications.

By critically evaluating the applicability of these criteria in real-world scenarios, this study aims to propel the advancements in welding technology and foster the development of precise and dependable fatigue assessment methods. The ultimate goal is to enhance the safety, efficiency, and sustainability of welded structures subjected to the demanding conditions of multiaxial fatigue loading. Through this exploration, valuable insights can be gained, ultimately driving the industry toward more resilient and optimized welding practices.

2 | FUNDAMENTALS OF EC AND IIW MULTIAXIAL FATIGUE ASSESSMENT CRITERIA

In the field of fatigue design, ECs and the IIW recommendations put forth two primary procedures: the safe life design method and the damage tolerant design method.[1–3] The safe life design method focuses on assessing the accumulation of damage throughout the structure's intended lifespan.[1–3] This evaluation involves a comparison between the maximum stress range and the CA limit, utilizing lower bound endurance data and an upper bound estimate of fatigue loading. By carefully selecting standard details and stress levels, this method guarantees consistent and reliable performance of the structure over its design life, eliminating the need for frequent in-service inspections to detect fatigue damage.[1–3]

In contrast, the damage-tolerant method requires regular inspection and maintenance throughout the structure's designated lifespan. This approach emphasizes the careful selection of suitable details, materials, and stress levels to minimize the rates of crack propagation and promote the development of lengthy critical crack lengths should cracks occur. Furthermore, the inclusion of multiple load paths and effective crack-arresting mechanisms is imperative within this method.[1–3] The primary emphasis of this paper is placed on the implementation of the safe life design method. The overarching objective is to provide practitioners with the essential knowledge and assessment techniques to design steel and aluminum welded joints.

When considering safe life design for CA fatigue loading, both ECs and the IIW offer comprehensive guidelines for evaluating welded joints subjected to multiaxial fatigue loading. These guidelines employ interaction equation fatigue assessment criteria, which are formulated based on normalized direct stress and shear stress ratios.[1–3] As per these standards, a welded joint is deemed safe if the cumulative damage remains below a predetermined threshold, which varies based on the material properties or the fatigue loading Conditions 1–3.

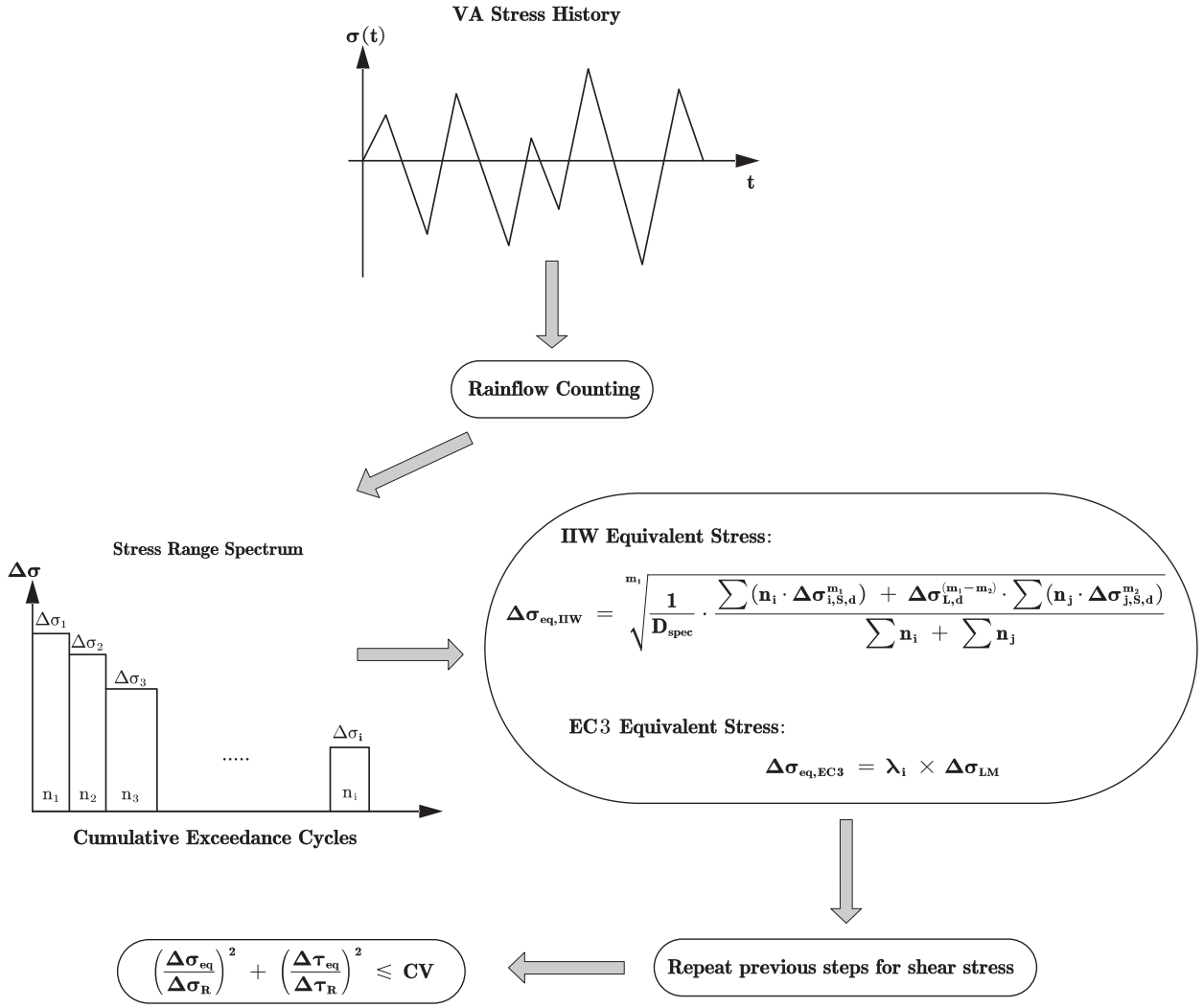

FIGURE 1 Design procedure for VA multiaxial fatigue loading using EC3 and IIW interaction equation criteria with equivalent stress range substitution.

Notably, Eurocode 9 (EC9) lacks an interaction equation that specifically considers normalized direct and shear stress ratios for multiaxial fatigue loading cases concerning aluminum welded joints.[2] Consequently, this review will concentrate exclusively on Eurocode 3 (EC3) for steel welded joints and the IIW recommendations for both aluminum and steel welded joints.[1,3] In the context of CA multiaxial fatigue loading, the interaction equations proposed by EC3 and the IIW are expressed as Equations (1) and (2), respectively[1,3]:

$$\left(\frac{\Delta\sigma_x}{\Delta\sigma_R/SF}\right)^3 + \left(\frac{\Delta\tau_{xy}}{\Delta\tau_R/SF}\right)^5 \leq D_{EC3}, \quad (1)$$

$$\left(\frac{\Delta\sigma_x}{\Delta\sigma_R/SF}\right)^2 + \left(\frac{\Delta\tau_{xy}}{\Delta\tau_R/SF}\right)^2 \leq D_{IIW}. \quad (2)$$

Table 1 provides a summary of the values of the allowable damage sums (i.e., D_{EC3} and D_{IIW}) under CA fatigue loading for different loading scenarios and materials. In Table 1, it can be observed that D_{EC3} is consistently equal to 1 for all loading cases, whereas D_{IIW} is 1 for in-phase fatigue loading and 0.5 for out-of-phase fatigue loading.[1,3] Besides that, the evaluation considers the application of a partial safety factor (SF) on the fatigue strength, in line with the recommendations of EC3 and the IIW. The rationale behind the selection of SF will be further discussed in the subsequent section.

For VA fatigue loading, two main approaches are recommended by ECs and the IIW: the interaction equation criterion and the linear damage accumulation Palmgren–Miner (P-M) rule.[1–3] These methods play a crucial role in assessing the fatigue strength and life of welded joints under VA loading scenarios. The interaction equation criterion, initially used for CA loading, remains relevant for VA loading, albeit with some significant distinctions. For VA loading, the applied stress range terms, $\Delta\sigma_x$ and $\Delta\tau_{xy}$ as employed in

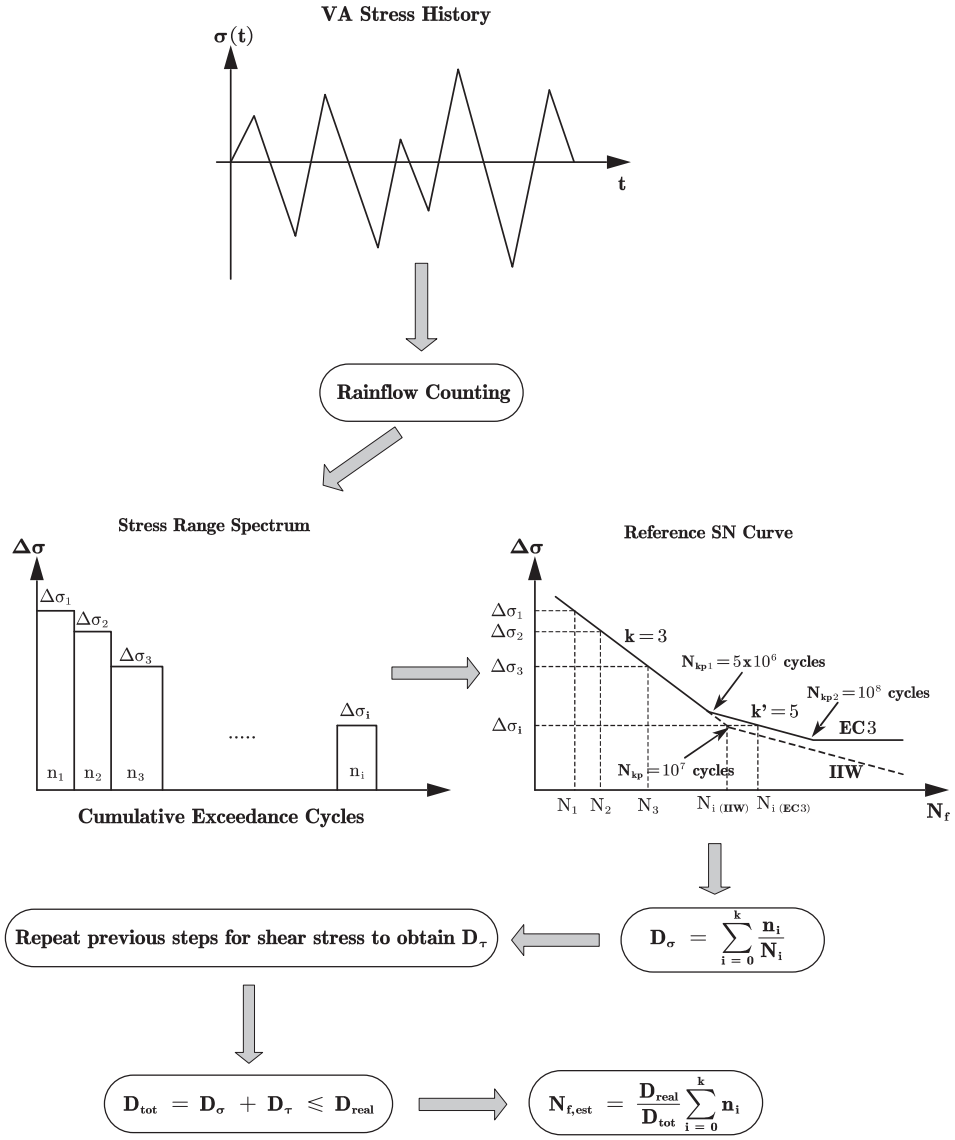

FIGURE 2 Design procedure for VA multiaxial fatigue loading using EC3 and IIW linear damage accumulation Palmgren–Miner (P-M) rule.

Equations (1) and (2), are replaced with equivalent stress range expressions, $\Delta\sigma_{eq}$ and $\Delta\tau_{eq}$ as denoted in Equations (3) and (4).[1–3]

$$\left(\frac{\Delta\sigma_{eq,\mathrm{EC3}}}{\Delta\sigma_R/SF}\right)^3+\left(\frac{\Delta\tau_{eq,\mathrm{EC3}}}{\Delta\tau_R/SF}\right)^5\le D_{\mathrm{EC3}} \tag{3}$$

$$\left(\frac{\Delta\sigma_{eq,\mathrm{IIW}}}{\Delta\sigma_R/SF}\right)^2+\left(\frac{\Delta\tau_{eq,\mathrm{IIW}}}{\Delta\tau_R/SF}\right)^2\le CV \tag{4}$$

Significantly, the allowable damage sum, which is applicable under CA loading for IIW's interaction criterion, undergoes a notable change when addressing VA loading. In this case, a comparison value (CV) is introduced, as outlined in Equation (4). The transition from D_{IIW} to CV when applying the IIW interaction equation criterion ensures a more tailored approach for VA conditions while maintaining the reliability of the overall design assessment.[3] Unlike the IIW interaction criterion, the EC3 interaction equation criterion under VA loading does not introduce a CV and retains the same allowable damage sum as CA loading (i.e., $D_{\mathrm{EC3}}=1$). The specific values for the allowable damage sums (i.e., D_{EC3} and D_{IIW}) and CV under various loading conditions for VA fatigue loading are also concisely presented in Table 1.[1–3]

EC3 adopts a simplified approach to determine the equivalent stress range, $\Delta\sigma_{eq,\mathrm{EC3}}$, which involves multiplying the maximum stress range that varies depending on the load model, $\Delta\sigma_{LM}$ with an equivalent damage factor, λ_i, as demonstrated in Equation (5)[1]:

$$\Delta\sigma_{eq,\mathrm{EC3}}=\lambda_i\times\Delta\sigma_{LM} \tag{5}$$

The λ_i factor varies based on load conditions and structural characteristics, with different applications, such as cranes and bridges, requiring distinct λ_i values to

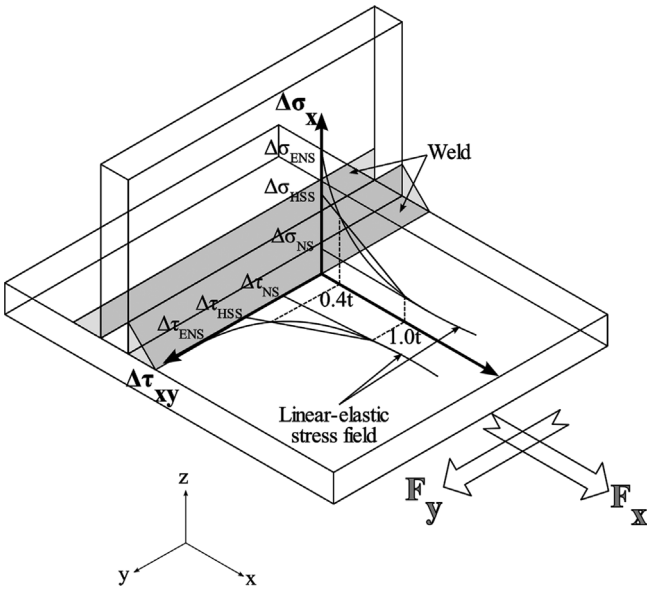

FIGURE 3 Overview of distinct stress analysis approaches—nominal stress (NS), hot spot stress (HSS), and effective notch stress (ENS)

meet specific design requirements.[1] In cases where λ_i is unknown, it is advisable to utilize the alternative P-M rule as the criterion for multiaxial fatigue assessment under VA fatigue loading.[1] In contrast, the IIW directly derives the equivalent stress range, $\Delta\sigma_{eq,\mathrm{IIW}}$ from Equation (6)[3]:

$$\Delta\sigma_{eq,\mathrm{IIW}} = \sqrt[m_1]{\frac{1}{D_{spec}} \cdot \frac{\sum\left(n_i \cdot \Delta\sigma_{i,S,d}^{m_1}\right) + \Delta\sigma_{L,d}^{(m_1-m_2)} \cdot \sum\left(n_j \cdot \Delta\sigma_{j,S,d}^{m_2}\right)}{\sum n_i + \sum n_j}}, \tag{6}$$

where

D_{spec}	Specified Miner sum
m_1	Slope above the knee point of the SN curve
m_2	Slope below the knee point of the SN curve
$\Delta\sigma_{i,S,d}$	Applied stress ranges above the knee point
$\Delta\sigma_{j,S,d}$	Applied stress ranges below the knee point
$\Delta\sigma_{L,d}$	Applied stress range at the knee point of the SN curve
n_i	Number of cycles at applied stress range $\Delta\sigma_i$
n_j	Number of cycles at applied stress range $\Delta\sigma_j$

The same formulations shown in Equations (5) and (6) can effectively be used to compute the shear stress ranges, by simply replacing $\Delta\sigma$ with $\Delta\tau$.[1,3] It is noteworthy to mention that the alternative equation proposed in the IIW guidelines, designed to address stress levels below the knee point, may be redundant.[4] This is because Equation (6), derived from applying the P-M rule with the modifications of Haibach, has demonstrated effectiveness in handling spectrum loading both above and below the knee point across the entirety of the S–N curve, accounting for slopes m_1 and m_2.[4,5]

Figure 1 illustrates the step-by-step process of implementing EC3 and IIW interaction equation criteria with the equivalent stress range substitution under VA loading.[1,3] Graphs can be utilized to visually depict the underlying principles of the interaction equations as shown in Equations (1)–(4). These graphical representations offer designers a clear visualization of the safety level attained by the designed welded joints. By employing the interaction criteria suggested by EC3 and IIW, designers can define a specific safety fatigue life or desired number of cycles to failure, typically recommended as 2 million cycles to failure.[1,3] The reference stresses corresponding to this threshold of 2 million cycles are recalculated, taking into account an appropriate probability of survival and additional SFs.[1,3] The selection of these factors is guided by standards that consider various geometries and welding configurations outlined in the codes.[1,3]

Interpreting reanalyses graphs accurately is essential for an accurate assessment. It is important to understand that points falling within the curve or boundary are deemed safe, signifying that the designed welded joint will endure for 2 million cycles or beyond.[1,3] On the contrary, points located outside the boundary indicate unsafe designs that will have a lifespan of fewer than 2 million cycles. The distance of points from the boundary serves as an indicator of the estimated number of cycles to failure, with a greater distance suggesting that the welded joint can only survive significantly fewer cycles than the 2 million cycle threshold. On the other hand, points situated within the boundary but significantly distant from it imply that the specimen has the capacity to withstand significantly more than 2 million cycles.

Unlike other multiaxial stress assessment criteria, such as the critical plane approach, the interaction equations proposed by EC3 and the IIW do not offer direct estimations of the number of cycles to failure.[6–22] As the original formulations of both EC3 and the IIW interaction equations lack the provision for deriving the estimated number of cycles to failure, only interaction diagrams are provided instead of fatigue life graphs. These fatigue life graphs can only be obtained by applying the modified P-M rule for VA loading cases. It is important to note that alternative formulations of the interaction equations exist, which allow for the estimation of cycles to failure using effective stress ranges.[11,14,15] However, since these alternative formulations are not explicitly recommended by EC3 and the

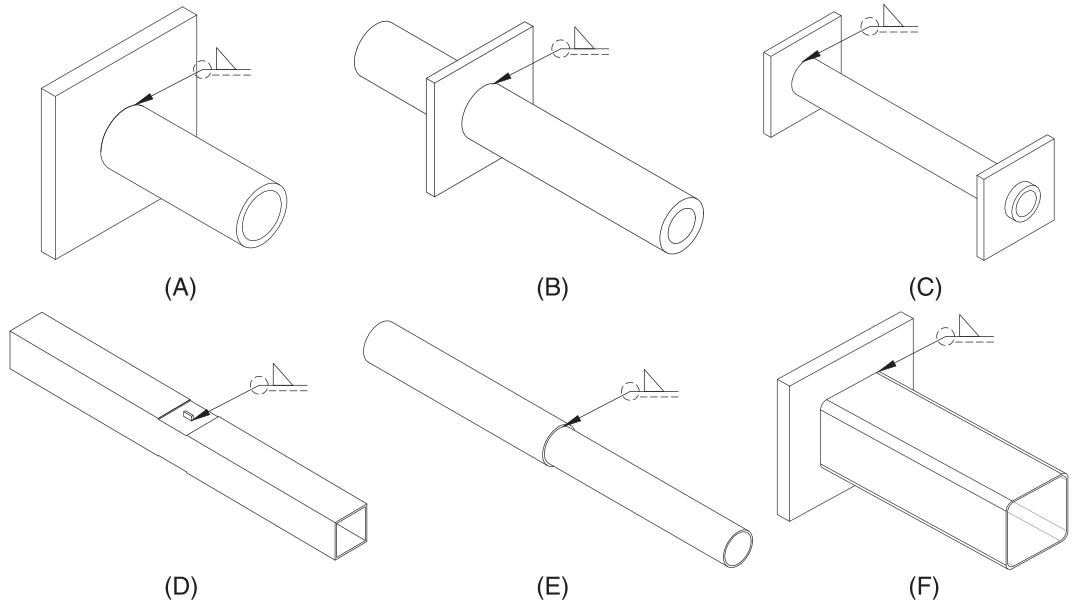

FIGURE 4 Geometries of the reviewed welded joints.

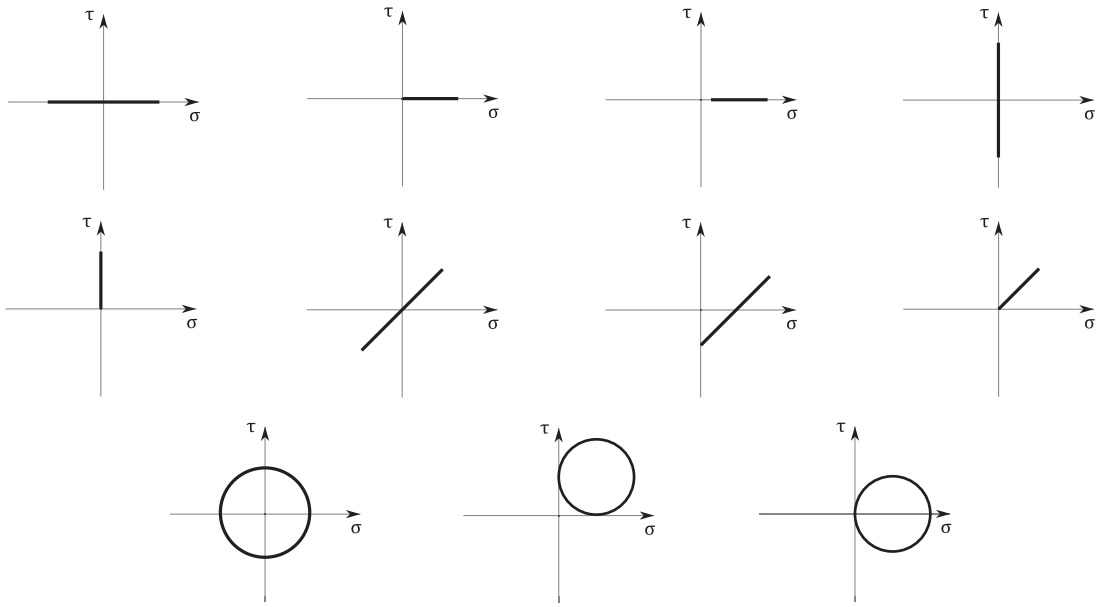

FIGURE 5 Loading paths.

IIW, they will not be utilized in this review when reanalyzing fatigue data to validate the reliability of the multiaxial fatigue assessment criteria proposed by EC3 and IIW.[1,3]

Another approach to address VA fatigue loading scenarios is the modified P-M rule,[1–3] also commonly known as the linear damage accumulation rule. It calculates the total damage, D_{tot}, accumulated by the welded joint and it can be obtained by summing up the damages caused by direct stresses and shear stresses, based on the applied stress levels, as expressed in Equation (7):

$$D_{tot} = D_\sigma + D_\tau \leq D_{real}. \tag{7}$$

The rainflow cycle counting method is employed to determine the number of cycles at the applied stress levels, n_i. Once the load spectrum is obtained, it can be matched directly with the standard EC3 and IIW reference S–N curves to extrapolate the corresponding

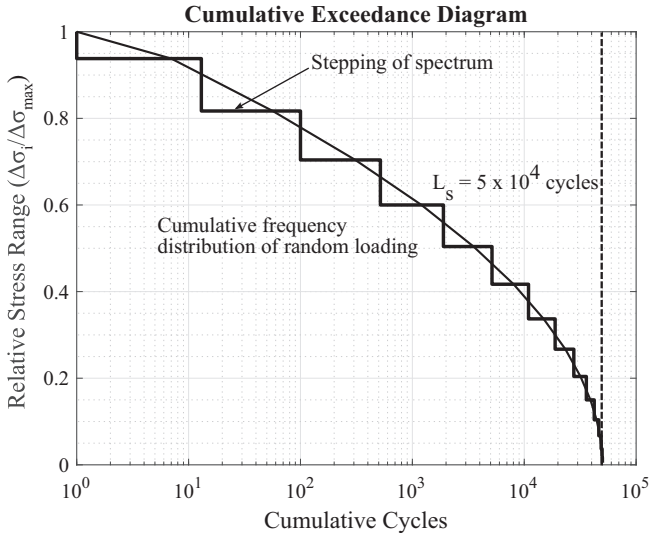

FIGURE 6 Variable amplitude (VA) Gaussian loading spectrum.

TABLE 2 Matrix of safety factors (SFs) for assessment methods and failure consequence levels.

	Consequence of failure	
Assessment method	**Low**	**High**
Damage tolerant	1.00	1.15
Safe life	1.15	1.35

Note: The safety factors reduce allowable FAT values for the probability of survival (Ps) = 97.7%.

number of cycles to failure, N_i.[1–3] Consequently, individual values of D_σ or D_τ can be derived using the following equation:

$$D_\sigma\,(\text{or}\,D_\tau) = \sum_{i=0}^{k} \frac{n_i}{N_i}. \tag{8}$$

The modified P-M rule assumes that fatigue failure occurs when the damage fraction of fatigue life reaches or exceeds the real damage sum, D_{real}, as shown in Equation (8). It is important to highlight that as opposed to the original P-M rule which suggests an allowable damage sum, D_{al}, of 1, different research studies have demonstrated that the real damage sum for steel and aluminum scatters between 0.01 and 10.[23,24] Consequently, a value of $D_{\text{al}} = 0.5$, with a probability of occurrence of 50% has been established as an engineering compromise for estimating fatigue life.[23–25] This modification was incorporated into the IIW recommendations.[3,26] With this concept, the estimated number of cycles to failure, $N_{\text{f,e}}$, can be determined by utilizing D_{real} and D_{tot}, attributed to multiaxial fatigue loading, as calculated using Equation (9):

$$N_{\text{f,e}} = \frac{D_{\text{real}}}{D_{\text{tot}}} \sum_{i=0}^{k} n_i. \tag{9}$$

The implementation process of the P-M rule, following the guidelines provided by ECs and the IIW, is depicted in Figure 2.[1–3] Consequently, the estimations are then visually presented on fatigue life graphs, plotting the experimental number of cycles to failure, N_{f}, against the estimated number of cycles to failure, $N_{\text{f,e}}$, encompassed within the uniaxial and torsional scatter bands. This graphical representation illustrates the accuracy and reliability of the estimations. It is essential to note that when employing the P-M rule as per EC3 and the IIW recommendations, the applied stress ranges are expressed in terms of direct stress ranges and shear stress ranges for computing the damage sum.[1,3] However, in the case of EC9, the VA stress ranges are represented in terms of maximum principal stresses.[2] This distinction should be considered when evaluating fatigue life estimations using the respective standards.

3 | VALIDATION METHOD OF EC3 AND IIW INTERACTION EQUATION CRITERIA

In this comprehensive quantitative review, the recommended EC3 and IIW interaction equation criteria are thoroughly evaluated through a reanalysis of extensive fatigue data under CA and VA fatigue loading compiled from the literature.[18,27–43] The assessment incorporates the integration of different stress analysis approaches, including the nominal stress (NS), hot spot stress (HSS), and effective notch stress (ENS) methods.[1–3,15,22,44–51] By combining these analyses, valuable insights into the accuracy and conservatism of these criteria are gained, providing a deeper understanding of their practical effectiveness in assessing multiaxial fatigue. To visually illustrate the application and distinctions of each stress analysis approach, Figure 3 provides a concise representation of a weld seam under tension and shear.

Additionally, Figure 4 showcases the geometries of the steel and aluminum welded joints being examined, highlighting important characteristics.[18,27–43] Notably, the weld leg sizes range from 0.8 to 11 mm, with the plate thickness varying between 1.5 and 10 mm. Moreover, the length of these welded joints spans from 107.5 to 2040 mm. This range of dimensions provides valuable

TABLE 3 Summary of reanalyzed welded joints using NS approach under CA and interaction equation criterion under VA fatigue loading, including uniaxial and torsional reference fatigue strengths, geometries, materials, fatigue curve slopes, and data sources.

Material	$\Delta\sigma_{R,Ps=97.7\%}$[a] (MPa)			Uniaxial curve slope, k					$\Delta\tau_{R,Ps=97.7\%}$[a] (MPa)			Torsional curve slope, $k0$				Geometry	Reference
				k (before the first knee point)[b]		k^* (after the first knee point)[b]		k^* (after the second knee point)[c]				$k0$ (before knee point)[d]		$k0^*$ (after knee point)[d]			
(CA)	EC3	IIW	Exp[e]	EC3/ IIW	Exp[e]	EC3	IIW	EC3	EC3	IIW	Exp[d]	EC3/ IIW	Exp[e]	EC3	IIW		
UM StE 460[h]	71	71	142.7	3	4.4	5	22	∞	100	100	127.5	5	4.9	∞	22	Figure 4A	[27]
M StE 460[h]	71	71	166.5	3	4.6	5	22	∞	100	100	-	5	-	∞	22	Figure 4A	[30]
UM StE 460[h]	71	71	194.7	3	4.4	5	22	∞	100	100	-	5	-	∞	22	Figure 4E	[30]
M StE 460[h]	71	71	321.6	3	8.2	5	22	∞	100	100	128	5	6.3	∞	22	Figure 4E	[30]
StE 460[h]	71	71	116.4	3	3.9	5	22	∞	100	100	180.9	5	7.3	∞	22	Figure 4A	[37]
StE 460	71	71	122.9	3	5.4	5	22	∞	100	100	80.5	5	6.1	∞	22	Figure 4A	[39]
A519	71	71	96.3	3	5.4	5	22	∞	80	80	94.2	5	3.7	∞	22	Figure 4B	[36]
A519-A36[h]	80	80	144.4	3	3.8	5	22	∞	100	100	104.2	5	5.5	∞	22	Figure 4D	[35]
BS4360 Gr.50E	71	71	65.6	3	3	5	22	∞	80	80	66.3	5	4.5	∞	22	Figure 4C	[43]
Fe 52 steel	45	45	15.8	3	2.3	5	22	∞	100	100	44.1	5	3.5	∞	22	Figure 4F	[40]
BS4360	80	80	-	3	-	5	22	∞	80	80	-	5	-	∞	22	Figure 4D	[38]
S340 + N, E355 + N	71	71	204.2	3	6.1	5	22	∞	100	100	207.8	5	6.6	∞	22	Figure 4E	[41]
S340 + N, E355 + N[h]	71	71	44.6	3	2.9	5	22	∞	100	100	71.3	5	3.6	∞	22	Figure 4E	[41]
St 35 ($t = 1$ mm)	71	71	69.2	3	4.9	5	22	∞	100	100	106.4	5	8.4	∞	22	Figure 4E	[33]
St 35 ($t = 2$ mm)	71	71	66.4	3	5.3	5	22	∞	100	100	74.5	5	6.1	∞	22	Figure 4E	[31]
6082-T6	N/C[f]	32	55	3	6.9	5	22	∞	N/C[f]	36	50.4	5	6.2	∞	22	Figure 4A	[18]
6060-T6[h]	N/C[f]	22	-	3	-	5	22	∞	N/C[f]	36	-	5	-	∞	22	Figure 4E	[42]
AW 6082	N/C[f]	22	20.3	3	4.2	5	22	∞	N/C[f]	36	42.3	5	5.8	∞	22	Figure 4E	[33]
AW 5042	N/C[e]	22	16.6	3	4.1	5	22	∞	N/C[e]	36	42.5	5	5.9	∞	22	Figure 4E	[33]

TABLE 3 (Continued)

Material	$\Delta\sigma_{R,Ps=97.7\%}$[a] (MPa)			Uniaxial curve slope, k				$\Delta\tau_{R,Ps=97.7\%}$[a] (MPa)			Torsional curve slope, $k0$				Geometry	Reference
				k (before the first knee point)[b]		k^* (after the first knee point)[b]		k^* (after the second knee point)[c]				$k0$ (before knee point)[d]		$k0^*$ (after knee point)[d]		
(CA)	EC3	IIW	Exp[e]	EC3/IIW	Exp[e]	EC3	IIW	EC3	EC3	IIW	Exp[d]	EC3/IIW	Exp[e]	EC3	IIW	
Material	$\Delta\sigma_{R,Ps=97.7\%}$[a] (MPa)			Uniaxial curve slope, k					$\Delta\tau_{R,Ps=97.7\%}$[a] (MPa)			Torsional curve slope, $k0$				Geometry	Reference
				k (before the first knee point)[b]		k' (before the first knee point)[b]		k' (after the second knee point)[c]				$k0$ (before knee point)[d]		$k0'$ (after knee point)[d]		
(VA)	EC3		IIW	EC3/IIW		EC3	IIW[g]	EC3	EC3		IIW	EC3/IIW		EC3	IIW[g]	
StE 460[h]	71		71	3		5	5	∞	100		100	5		∞	9	Figure 4A	[34]
StE 460[h]	71		71	3		5	5	∞	100		100	5		∞	9	Figure 4A	[37]
42CrMo4[h]	-		-	-		-	-	-	100		100	5		∞	9	Figure 4E	[28]
6082-T6	N/C[f]		32	3		5	5	∞	N/C[f]		36	5		∞	9	Figure 4A	[29]

Abbreviations: M, machined; UM, unmachined.

[a]Reference normal and shear stresses extrapolated at 2 million cycles to failure, with a probability of survival (Ps) = 97.7%.

[b]The first knee point for the IIW and EC3 in terms of normal stress is located at the number of cycles to failure (N_{kp}) = 10^7 cycles and (N_{kp}) = 5×10^6 cycles, respectively.

[c]The second knee point for EC3 in terms of normal stress is located at $N_{kp} = 10^8$ cycles.

[d]The knee point for both the IIW and EC3 in terms of shear stress is located at $N_{kp} = 10^8$ cycles.

[e]Exp denotes experimental data.

[f]N/C denotes not considered in the reanalysis.

[g]Slopes (k' and $k0'$) suggested by the IIW for VA loading are derived from Haibach's modification ($2k - 1$), where k is the slope before the knee point.

[h]Stress-relieved.

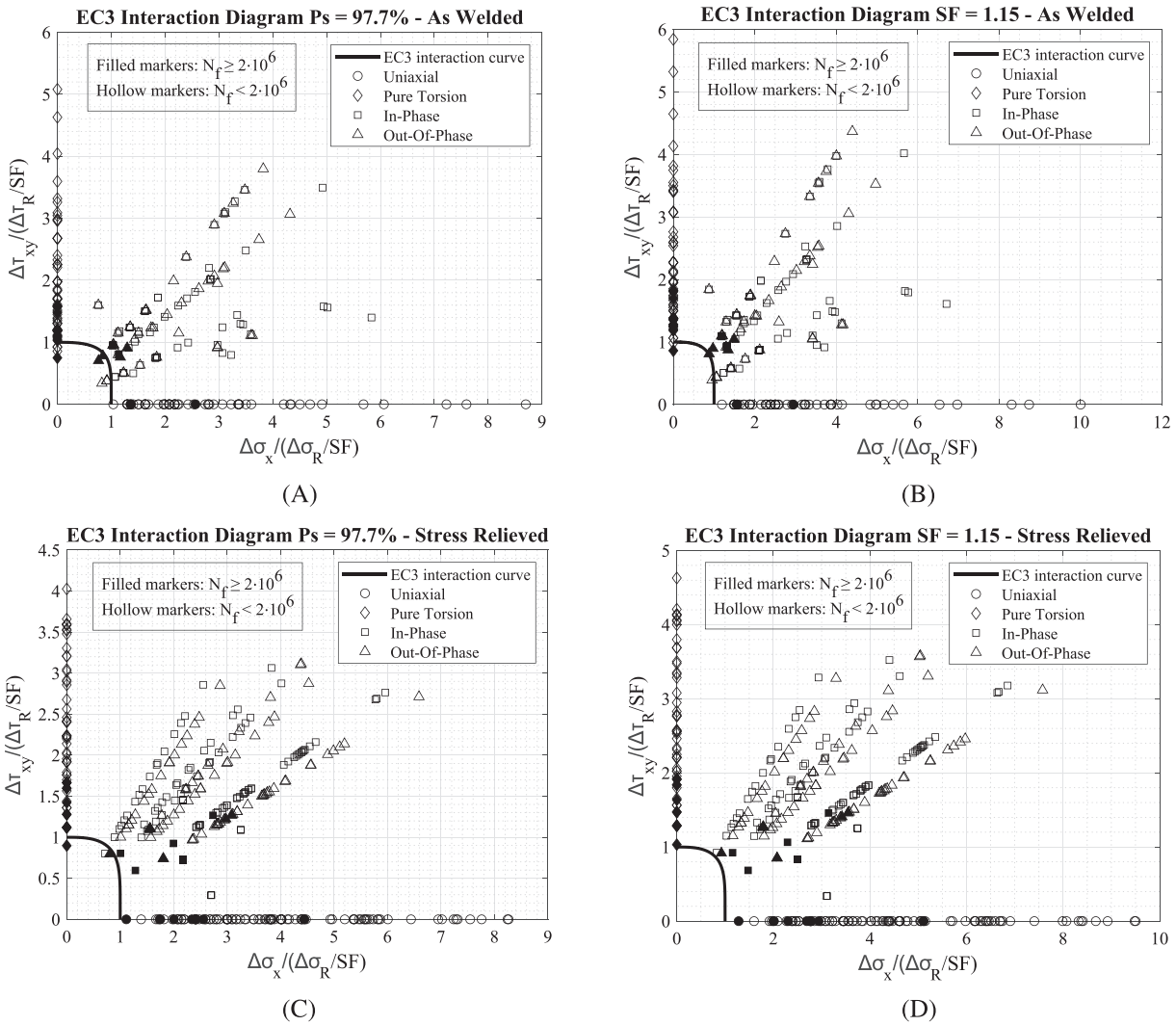

FIGURE 7 Nominal stress (NS) approach: EC3 interaction diagram for as-welded (A, B) and stress-relieved (C, D) **steel** welded joints under **CA** fatigue loading, with reference stresses ($\Delta\sigma_R$ and $\Delta\tau_R$) recalculated based on $Ps = 97.7\%$ and $SF = 1.15$.

insights into the diverse configurations considered in the analysis.

The reviewed fatigue data comprise CA fatigue testing conducted under diverse loading conditions, including bending, tension, and torsion. These tests encompass a range of loading scenarios, such as uniaxial, pure torsional, in-phase, and out-of-phase fatigue loading, with different load ratios ($R = \sigma_{min}/\sigma_{max}$ or $R = \tau_{min}/\tau_{max}$) such as $R = -1$, 0, and 0.1.[18,27,36–43] For CA fatigue loading, Figure 5 visually presents the loading paths for these fatigue tests, offering a clear depiction of the distinct loading profiles encountered in the literature. On the other hand, for VA fatigue loading, a Gaussian loading spectrum with a sequence length of 5×10^4 cycles was applied to all VA loading cases, as demonstrated in Figure 6.[27–29,37]

In assessing metal fatigue, particularly under axial loading, mean stress proves notably significant.[13,52] A key observation is that high tensional residual stresses can yield a local load ratio exceeding 0, even within an R range of −1 to 0.[53] To reduce the impact of residual stresses, heat treatments are applied for stress relief in welded joints. Consequently, these treatments have demonstrated an enhancement in the fatigue strength of welded joints.[13] Notably, many reanalyzed outcomes in this quantitative review are based on such stress-relieved joints. Given that design codes, in the case of stress-relieved steel and aluminum joints, consider worst-case scenarios involving high tensile residual stresses, a measured approach is adopted in the reanalysis. To avoid an undue level of conservatism, only 60% of the compressive stress range is incorporated,

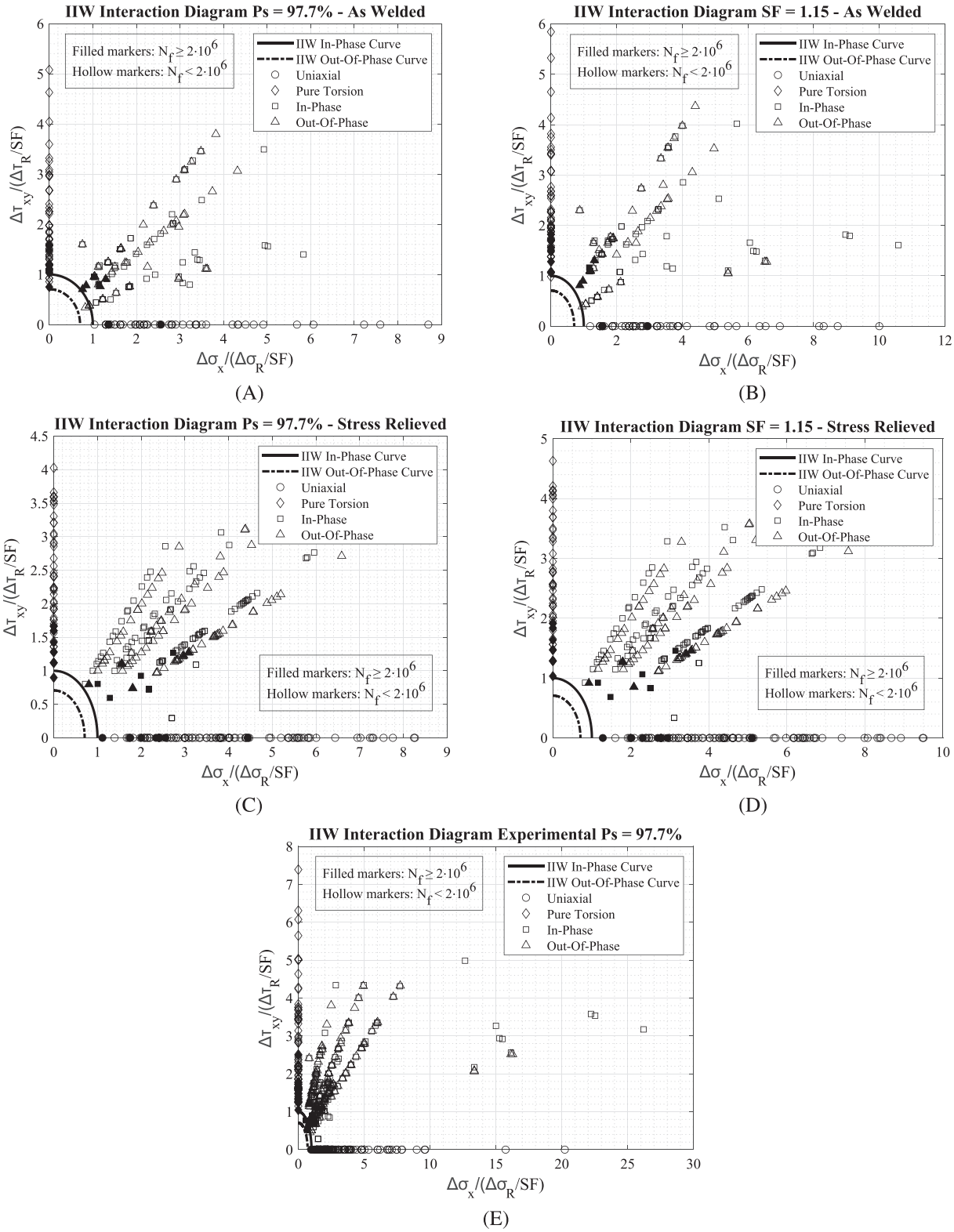

FIGURE 8 Nominal stress (NS) approach: IIW interaction diagram for as-welded (A, B) and stress-relieved (C, D) **steel** welded joints under **CA** fatigue loading, with reference stresses ($\Delta\sigma_R$ and $\Delta\tau_R$) recalculated based on $Ps = 97.7\%$, $SF = 1.15$, and experimental data.

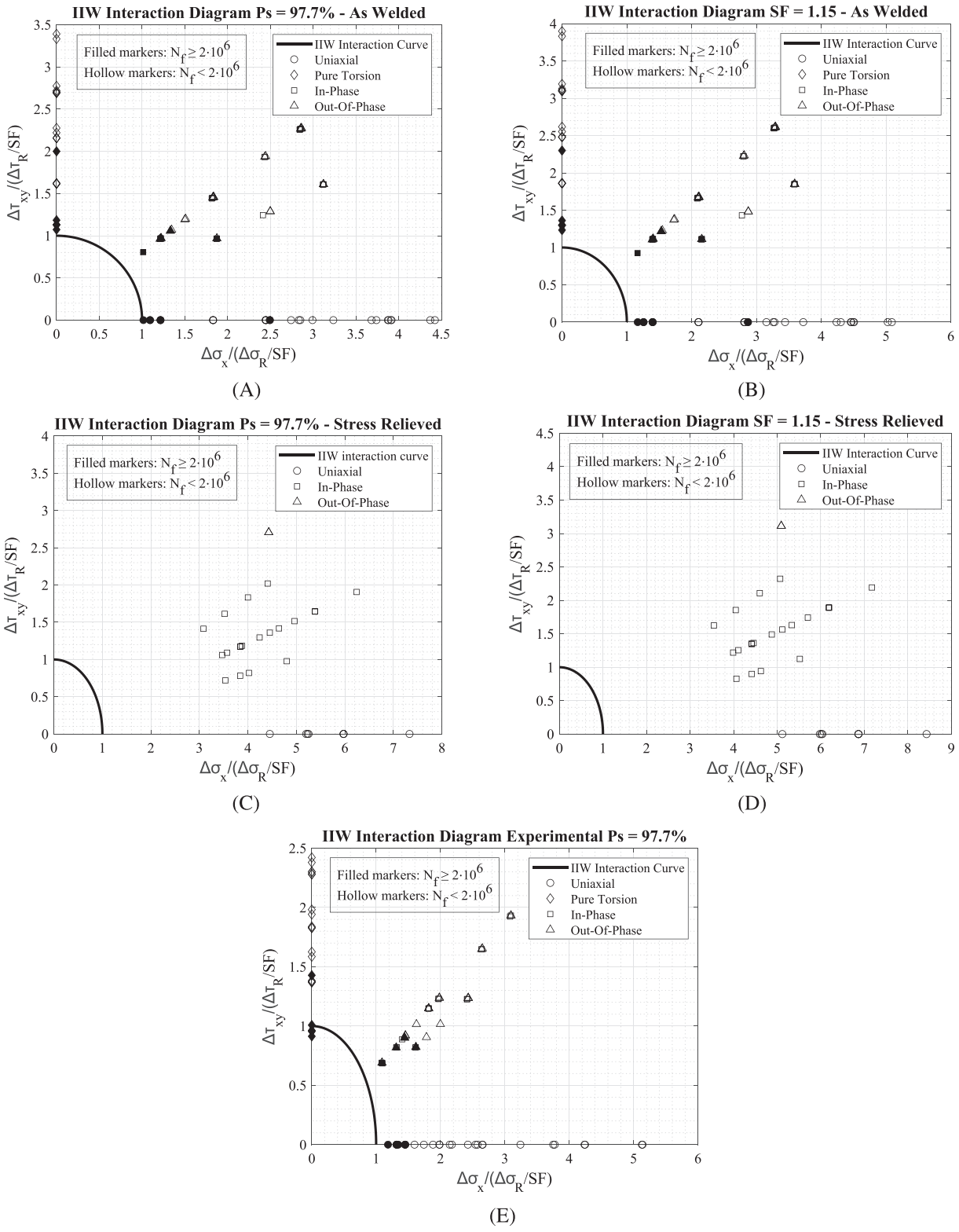

FIGURE 9 Nominal stress (NS) approach: IIW interaction diagram for as-welded (A, B) and stress-relieved (C, D) **aluminum** welded joints under **CA** fatigue loading, with reference stresses ($\Delta\sigma_R$ and $\Delta\tau_R$) recalculated based on $Ps = 97.7\%$, $SF = 1.15$, and experimental data.

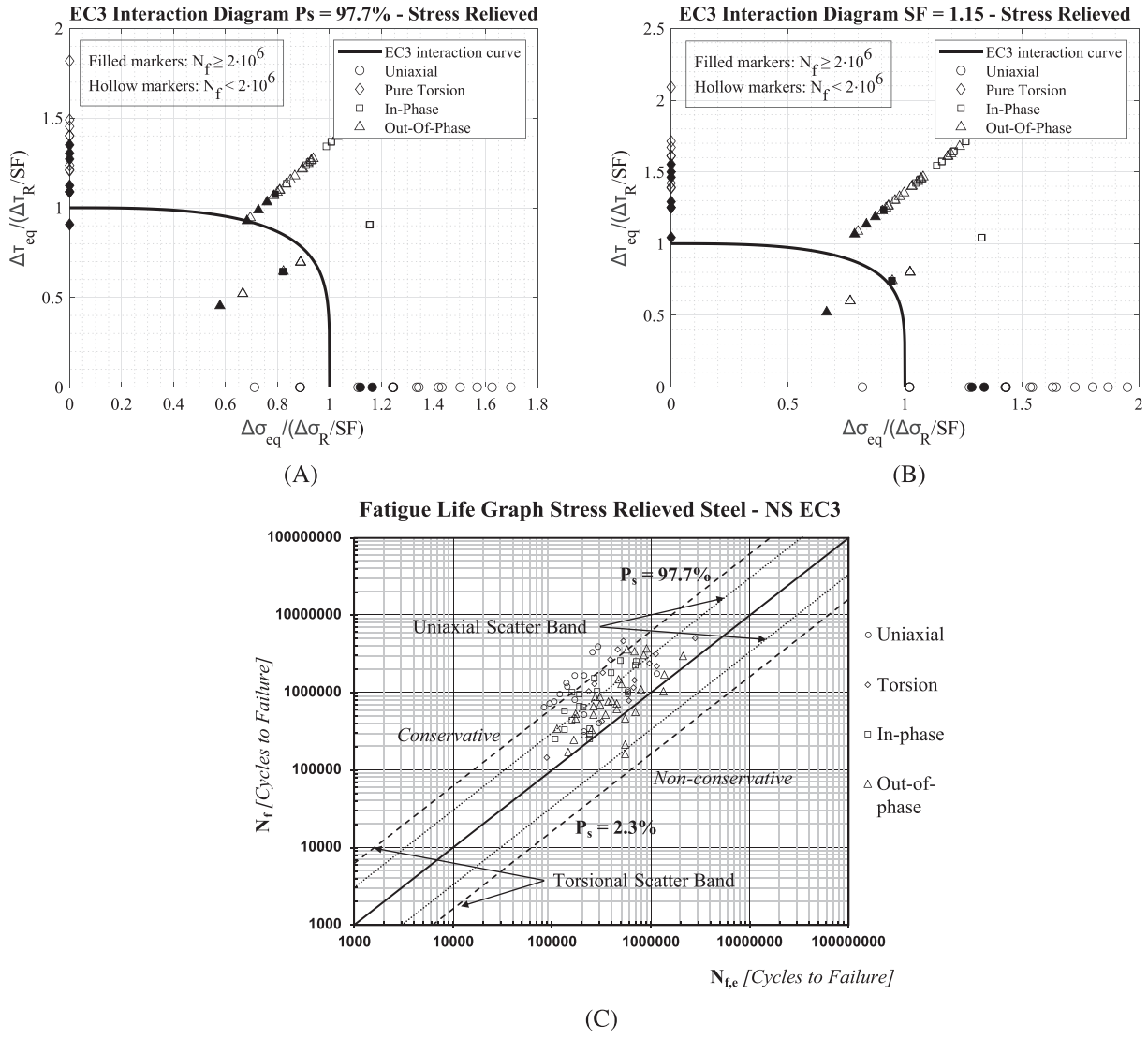

FIGURE 10 Nominal stress (NS) approach: EC3 interaction diagram (A, B) and fatigue life graph (C) for stress-relieved **steel** welded joints under **VA** fatigue loading, with reference stresses ($\Delta\sigma_R$ and $\Delta\tau_R$) recalculated based on $Ps = 97.7\%$ and $SF = 1.15$

aligning with the recommendations of both EC3 and the IIW[1,3]:

$$\Delta\sigma_{eff} = |\sigma_{max}| + 0.6\,|\sigma_{min}|. \tag{10}$$

This recommended approach, outlined in Equation (10), accounts for the positive impact of stress relief and contributes to a more accurate assessment of the stress distribution in welded joints.[1,3] The reanalysis process involves obtaining the reference stresses at 2 million cycles to failure from standard FAT values, which are determined based on the welding configuration and experimental fatigue data obtained from uniaxial and pure torsional tests. During the reanalysis, the reference stresses are recalculated at a probability of survival (*Ps*) of 97.7%, which corresponds to the mean minus two standard deviations. Although there is a conventional recommendation for *Ps* to be set at 95% with a two-sided confidence interval limit in various applications, the difference between $Ps = 97.7\%$ and $Ps = 95\%$ with a two-sided confidence level is less than 2%. This difference is considered negligible, especially when accounting for the inherent spread of fatigue data. Therefore, adopting *Ps* of 97.7% aligns with the recommendations of both EC3 and the IIW.[1,3] This approach ensures a consistent and dependable assessment of the reference stresses, facilitating a comprehensive evaluation of fatigue behaviour in accordance with industry standards.

As highlighted earlier, a partial SF is adopted when assessing the welded joints under multiaxial fatigue loading through the application Equations (1)–(4) as recommended by the IIW and EC3. Specifically, considering the low consequence of failure for the steel and aluminum welded joints under review, an SF of 1.15 is adopted

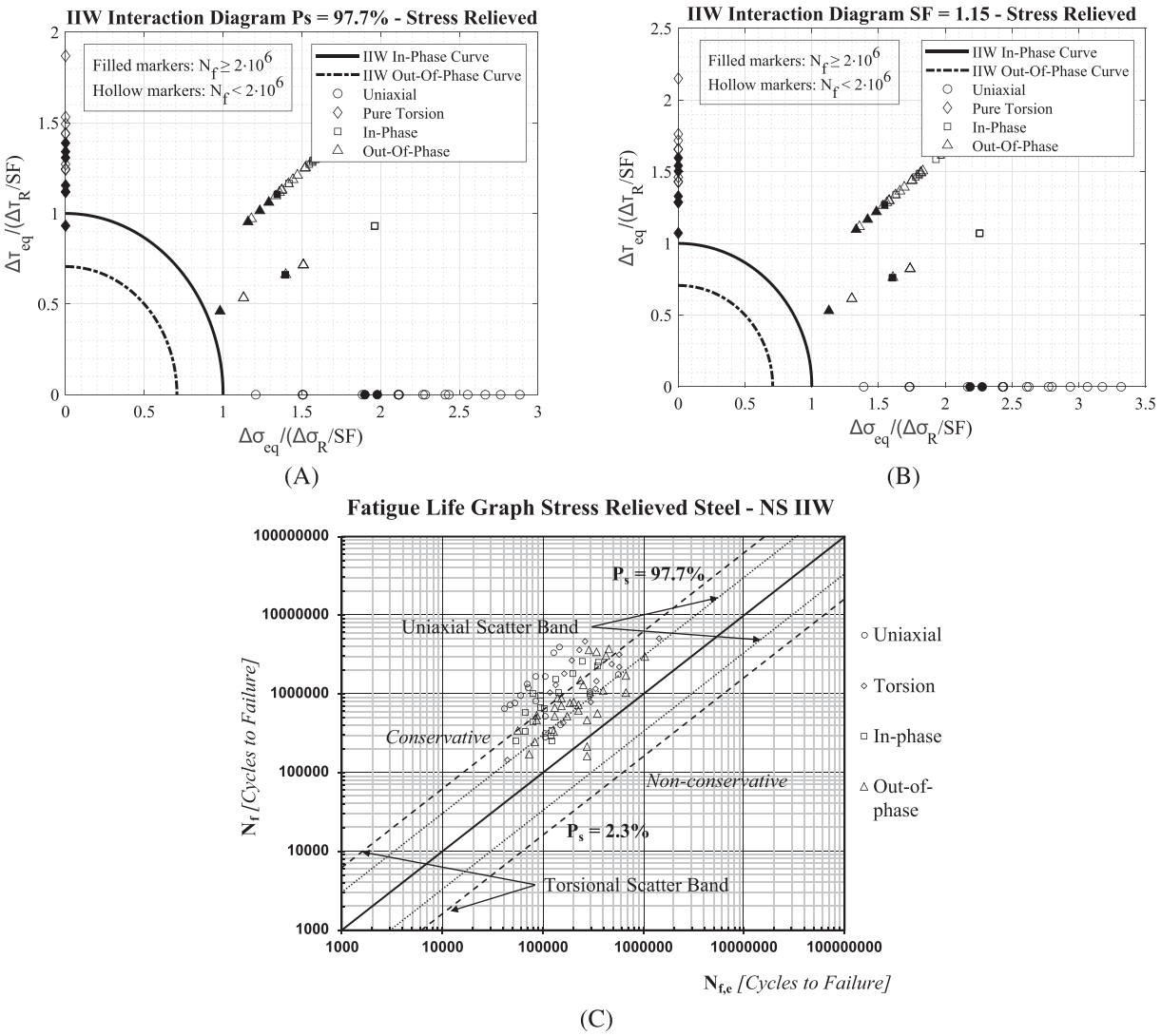

FIGURE 11 Nominal stress (NS) approach: IIW interaction diagram (A, B) and fatigue life graph (C) for stress-relieved **steel** welded joints under **VA** fatigue loading, with reference stresses ($\Delta\sigma_R$ and $\Delta\tau_R$) recalculated based on $Ps = 97.7\%$ and SF = 1.15.

within the safe life design method discussed earlier.[1,3] To provide a comprehensive overview, Table 2 presents a matrix of partial SF that accounts for various assessment methods and different levels of failure consequence. This ensures a robust approach to assessing the fatigue strength, considering the specific characteristics and potential consequences of failure for each welded joint configuration.

The distinction between EC3 and IIW becomes apparent when considering the exponent applied to the normalized direct stress and shear stress ratios. In EC3, the inclusion of the slope of the reference fatigue curve, which is set to 3 for uniaxial fatigue curves and 5 for torsional fatigue curves in Equation (1), adds complexity.[1] The challenge arises from the variations in experimental fatigue curves obtained from diverse literature sources, making it difficult to plot them on a single graph for an overall accuracy assessment of EC3. In contrast, the IIW interaction equation criteria, also known as the Gough–Pollard criterion, adopt a consistent exponent of 2 for the normalized direct and shear stress ratios, regardless of the fatigue curve slope.[3,54] Therefore, in the case of CA fatigue loading, the experimentally derived reference stresses solely rely on the IIW multiaxial fatigue assessment criteria, offering a reliable and standardized framework for analysis and comparisons.

The evaluation of VA loading using the P-M rule involves plotting the experimental, N_f, against the estimated, $N_{f,e}$, number of cycles to failure, providing insights into the accuracy and reliability of the criterion according to ECs and the IIW guidelines.[1–3] Since reference stresses for VA loading are recalculated at a $Ps = 97.7\%$, the estimations are expected to cluster around the uniaxial and torsional $Ps = 97.7\%$ line.[1–3,8,22]

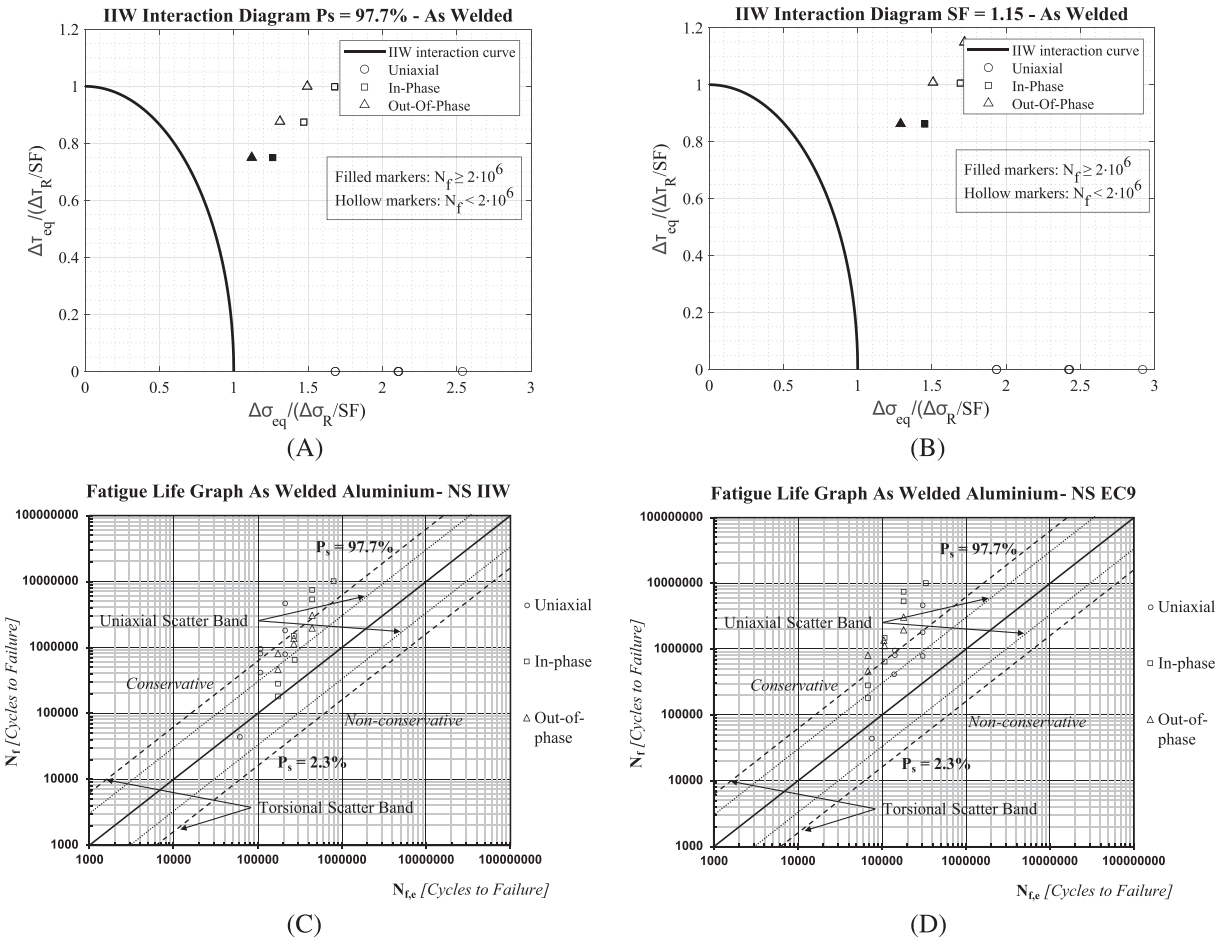

FIGURE 12 Nominal stress (NS) approach: IIW interaction diagram (A, B), IIW fatigue life graph (C), and EC9 fatigue life graph (D) for as-welded aluminum welded joints under VA fatigue loading, with reference stresses ($\Delta\sigma_R$ and $\Delta\tau_R$) recalculated based on $Ps = 97.7\%$ and $SF = 1.15$.

Ideally, most of the points or estimations should lie above the diagonal line where $Ps = 50\%$, indicating $N_f = N_{f,e}$. This alignment is crucial to demonstrate the accuracy and reliability of the P-M rule as a robust multiaxial fatigue assessment criterion for VA loading. Conversely, if the reference stresses were recalculated at $Ps = 50\%$, the estimations would primarily fall within the uniaxial and torsional scatter bands, offering further insights into the fatigue life estimations under VA loading conditions. These results play a pivotal role in validating and refining the fatigue assessment criteria for welded joints.

Similarly, the validation method and limitations discussed for CA loading are equally applicable when employing the interaction equation criterion for VA loading. However, it is crucial to acknowledge that there are differences in the number and location of knee points on the reference fatigue curves between the ECs and IIW standards for VA loading. The reference fatigue curves provided by ECs exhibit two knee points situated at $N_{kp1} = 5$ million cycles and at $N_{kp2} = 10^8$ cycles. As a result, three segments of straight lines with inverse slopes of 3, 5, and ∞ are formed.[1] In contrast, the standard IIW reference fatigue curves feature a single knee point at $N_{kp} = 10^7$ cycles, leading to two segments with inverse slopes of $k = 3$ and $k' = 5$ for the uniaxial S–N curve.[3] For the torsional S–N curve, the knee point is at $N_{kp} = 10^8$ cycles, yielding an inverse slope, $k0$ of 5 before the knee point and $k0'$ of 9 after the knee point, calculated based on Haibach's modification $(2k - 1)$, where k is the inverse slope before the knee point.[3,55] Conversely, under CA fatigue loading conditions, the inverse slopes, k^* and $k0^*$ after the knee point according to the IIW recommendations change to 22 for both uniaxial and torsional S–N curves.[3] These variations in curvature and slope between ECs and IIW recommendations should be considered when assessing fatigue life estimations under different loading conditions.

As explained earlier, EC3 suggests using simplified coefficient λ_i, which varies depending on the specific structural application and the type of loading conditions.

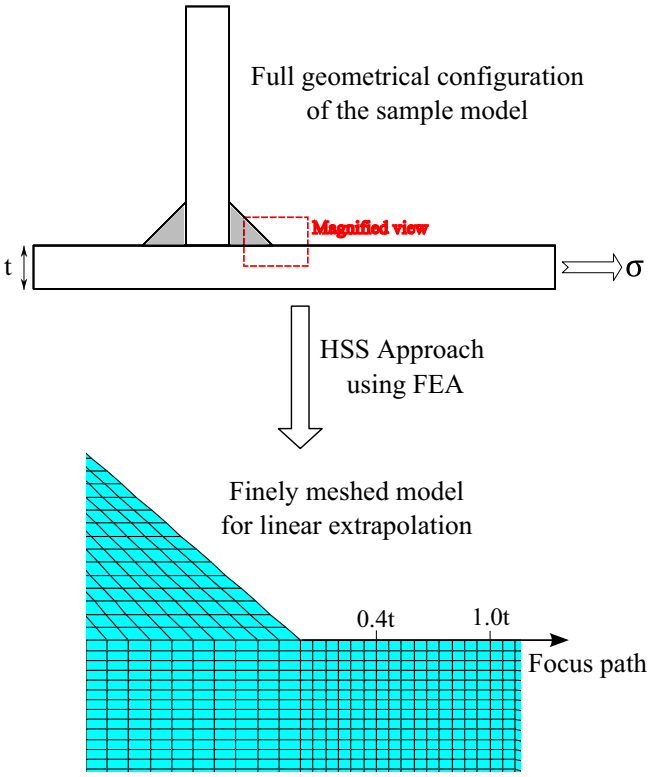

FIGURE 13 Example of finely meshed finite element (FE) model showcasing the application of hot spot stress (HSS) analysis approach. [Colour figure can be viewed at wileyonlinelibrary.com]

For instance, in crane structural applications, λ_i ranges from 0.198 to 1.587 for direct stresses and from 0.379 to 1.320 for shear stresses.[56] It should be noted that these variations are tailored to specific structural domains. Since the data under review serves scientific purposes without a specific target in mind within any particular structural domain, the least conservative λ_i values suggested for the crane domain will be utilized as an example case in the reanalysis using the EC3 interaction criterion for VA loading. Specifically, the lowest values, 0.198 for direct stress and 0.379 for shear stress, are adopted.[56] This deliberate choice aims to emphasize the importance of selecting appropriate values for λ_i and underscores the safety level associated with the recommended values for λ_i, with this holding particularly true in the context of the worst-case scenario when applying the EC3 interaction criterion for VA loading in a broader context. The accuracy and disparities between the ECs and IIW multiaxial fatigue assessment criteria will be thoroughly assessed by extensively analyzing their capabilities in predicting the fatigue life of welded joints through different stress analysis approaches. The upcoming sections of this paper will delve into these aspects, providing a comprehensive understanding of the topic.

4 | REANALYSES USING THE NOMINAL STRESS (NS) APPROACH

The NS approach is a widely accepted method used to analyze stress distributions in welded joints by considering the nominal cross-sectional area.[1,3,13,15,45,47] This approach is highly valued for its efficiency and practicality, particularly when dealing with standard and less complex welded joint geometries. The calculation of nominal stresses can be performed using bending and torsion equations derived from simple beam theory. Importantly, the NS approach effectively captures the influence of the overall macro geometry on stress distribution within the welded joint.[1,3,15,47]

Table 3 serves as a concise summary, effectively capturing the essential characteristics of the reanalyzed welded joints under CA loading using the NS approach. It provides a comprehensive overview that includes crucial information such as uniaxial and torsional reference fatigue strengths.

These fatigue strengths are derived from carefully selected reference fatigue curves sourced from relevant standards and experimental data. Additionally, the table offers detailed insights into the geometries of the welded joints, the materials investigated, the slopes of the fatigue curves, and their respective sources of data.

The reanalysis of the EC3 criterion applied in conjunction with the NS approach is visually presented in Figure 7 for both as-welded and stress-relieved steel welded joints under CA fatigue loading. The recalculations are carried out using $Ps = 97.7\%$ and $SF = 1.15$. Notably, the black-filled markers on the graph represent experimental fatigue life exceeding 2 million cycles. When these points fall within the curve or boundary, they indicate accurate estimations, demonstrating the ability to withstand more than 2 million cycles to failure. Conversely, if the filled points lie outside the curve or boundary, they are considered conservative estimates since the interaction equation criteria predict failure before reaching 2 million cycles, despite the specimens actually surviving beyond that threshold.

To quantitatively assess the level of conservatism, the percentage of non-conservative estimates (P_{NC}) is calculated. P_{NC} is determined by dividing the number of non-conservative estimates (i.e., the number of hollow markers within the interaction curve or boundary) by the total number of reanalyzed specimens, expressed as a percentage. The reanalysis reveals six instances of non-conservative estimates observed for as-welded steel joints, resulting in a P_{NC} of 2.54%. With an additional SF of 1.15, the number of non-conservative estimates reduces from 6 to 3 instances, which is equivalent to a P_{NC} of 0.85%. On the contrary, for stress-relieved steel

TABLE 4 Summary of reanalyzed welded joints using the HSS approach under CA and interaction equation criterion under VA fatigue loading, including uniaxial and torsional reference fatigue strengths, geometries, materials, fatigue curve slopes, and data sources

Material	$\Delta\sigma_{R,Ps=97.7\%}$[a] (MPa)			Uniaxial curve slope, k					$\Delta\tau_{R,Ps=97.7\%}$[a] (MPa)			Torsional curve slope, $k0$				Geometry	Reference
				k (before the first knee point)[b]		k^* (after the first knee point)[b]		k^* (after the second knee point)[c]				$k0$ (before knee point)[d]		$k0^*$ (after knee point)[d]			
(CA)	EC3	IIW	Exp[(5)]	EC3/ IIW	Exp[(5)]	EC3	IIW	EC3	EC3	IIW	Exp[d]	EC3/ IIW	Exp[(5)]	EC3	IIW		
UM StE 460[h]	90	90	188.7	3	4.4	5	22	∞	100	100	138.7	5	4.9	∞	22	Figure 4A	27
M StE 460[h]	90	90	210.0	3	4.6	5	22	∞	100	100	-	5	-	∞	22	Figure 4A	30
UM StE 460[h]	90	90	208.4	3	4.4	5	22	∞	100	100	-	5	-	∞	22	Figure 4E	30
StE 460[h]	90	90	163.1	3	3.9	5	22	∞	100	100	206.7	5	7.3	∞	22	Figure 4A	37
A519	90	90	112.7	3	5.4	5	22	∞	100	100	100.7	5	3.7	∞	22	Figure 4B	36
A519-A36[h]	90	90	153.6	3	3.8	5	22	∞	100	100	110.7	5	5.5	∞	22	Figure 4D	35
BS4360 Gr.50E	90	90	111.7	3	3	5	22	∞	100	100	72.7	5	4.5	∞	22	Figure 4C	43
Fe 52 steel	90	90	22.7	3	2.3	5	22	∞	100	100	48.4	5	3.5	∞	22	Figure 4F	40
S340 + N, E355 + N	90	90	343.0	3	6.1	5	22	∞	100	100	229.2	5	6.6	∞	22	Figure 4E	41
S340 + N, E355 + N[h]	90	90	74.8	3	2.9	5	22	∞	100	100	74.8	5	3.6	∞	22	Figure 4E	41
6082-T6	N/ C[f]	36	76.1	3	6.9	5	22	∞	N/ C[f]	36	55.0	5	6.2	∞	22	Figure 4A	18
6060-T6[h]	N/ C[f]	36	-	3	-	5	22	∞	N/ C[f]	36	-	5	-	∞	22	Figure 4E	42
Material	$\Delta\sigma_{R,Ps=97.7\%}$[a] (MPa)			Uniaxial curve slope, k					$\Delta\tau_{R,Ps=97.7\%}$[a] (MPa)			Torsional curve slope, $k0$				Geometry	Reference
				k (before the first knee point)[b]		k' (before the first knee point)[b]		k' (after the second knee point)[c]				$k0$ (before knee point)[d]		$k0'$ (after knee point)[d]			
(VA)	EC3		IIW	EC3/IIW		EC3	IIW[g]	EC3	EC3		IIW	EC3/IIW		EC3	IIW[g]		
StE 460[h]	90		90	3		5	5	∞	100		100	5		∞	9	Figure 4A	[34]

(Continues)

TABLE 4 (Continued)

Material	$\Delta\sigma_{R,Ps=97.7\%}$ (MPa)[a]	Uniaxial curve slope, k			$\Delta\tau_{R,Ps=97.7\%}$ (MPa)[a]	Torsional curve slope, $k0$			Geometry	Reference
		k (before the first knee point)[b]	k^* (after the first knee point)[b]	k^* (after the second knee point)[c]		$k0$ (before knee point)[d]		$k0^*$ (after knee point)[d]		
StE 460[h]	90	3	5	∞	100	5		∞	Figure 4A	37
	90	3	5	∞	100	5		∞	Figure 4A	37
42CrMo4[h]	-	-	-	-	100	5		∞	Figure 4E	28
	-	-	-	-	100	5		∞	Figure 4E	28
6082-T6	N/C[f]	3	5	∞	N/C[f]	5		∞	Figure 4A	29
	36	3	5	∞	36	5		∞	Figure 4A	29

Abbreviations: M, machined; UM, unmachined.
[a]Reference normal and shear stresses extrapolated at 2 million cycles to failure, with a probability of survival (Ps) = 97.7%.
[b]The first knee point for the IIW and EC3 in terms of normal stress is located at the number of cycles to failure (N_{kp}) = 10^7 cycles and (N_{kp}) = 5×10^6 cycles, respectively.
[c]The second knee point for EC3 in terms of normal stress is located at $N_{kp} = 10^8$ cycles.
[d]The knee point for both the IIW and EC3 in terms of shear stress is located at $N_{kp} = 10^8$ cycles.
[e]Exp denotes experimental data.
[f]N/C denotes not considered in the reanalysis.
[g]Slopes (k' and $k0'$) suggested by the IIW for VA loading are derived from Haibach's modification ($2k - 1$), where k is the slope before the knee point.
[h]Stress-relieved.

joints, only one non-conservative estimate is identified when the reference stresses are recalculated at $Ps = 97.7\%$, resulting in an overall P_{NC} of 0.28%, and by incorporating an additional SF of 1.15, the P_{NC} reduces to 0% as shown in Figure 7C,D.

Shifting our attention to the reanalysis of the IIW criteria using the NS approach, Figure 8 illustrates the results for steel welded joints, while Figure 9 displays the reanalysis outcomes for aluminum welded joints under CA loading. The reference stresses for both as-welded and stress-relieved steel joints are recalculated using $Ps = 97.7\%$, $SF = 1.15$, and experimental data.

Notably, when considering the IIW criteria, a significant observation emerges: the non-conservative estimates are lesser as compared to the reanalysis results obtained from the EC3 criteria, especially when focusing on the as-welded steel joints.

However, a significant degree of conservatism is observed in the reanalysis of aluminum welded joints, as all data points are considerably distant from the curve boundary that defines the design safety level. This observation holds true for both as-welded and stress-relieved cases. Nevertheless, when using experimentally derived reference stresses, the level of conservatism is slightly reduced, with data points approaching closer to the boundary curve compared to the reference stresses recommended by the IIW standard fatigue curves.

On the other hand, Table 3 also provides a concise overview of the investigated welded joints for VA loading, presenting their uniaxial and torsional fatigue curves derived from relevant reference fatigue curves based on EC3 and IIW assessment criteria. The table includes vital information about the welded joint geometries, materials, fatigue curve slopes, and their respective literature references.

Figure 10 displays the graphs for stress-relieved steel welded joints under VA fatigue loading, using the EC3 multiaxial fatigue assessment criteria with the NS approach. The recalculations are based on $Ps = 97.7\%$ and $SF = 1.15$ for consistency. In this case, the steel welded joints exhibit 9 instances of non-conservative estimates, leading to a P_{NC} of 11.1% when applying the EC3 interaction equation criterion with equivalent stress range substitution. Upon applying an additional $SF = 1.15$, the number of non-conservative estimates decreased from 9 to 3 instances, resulting in a P_{NC} of 3.7% of the total estimations. Importantly, the fatigue life estimations are primarily situated within the uniaxial and torsional scatter band, positioned above the $N_f = N_{f,e}$ diagonal line. This alignment indicates accurate and conservative estimations in line with the EC3 P-M rule.

Figure 11 showcases reanalysis results for steel welded joints under VA loading, using the IIW

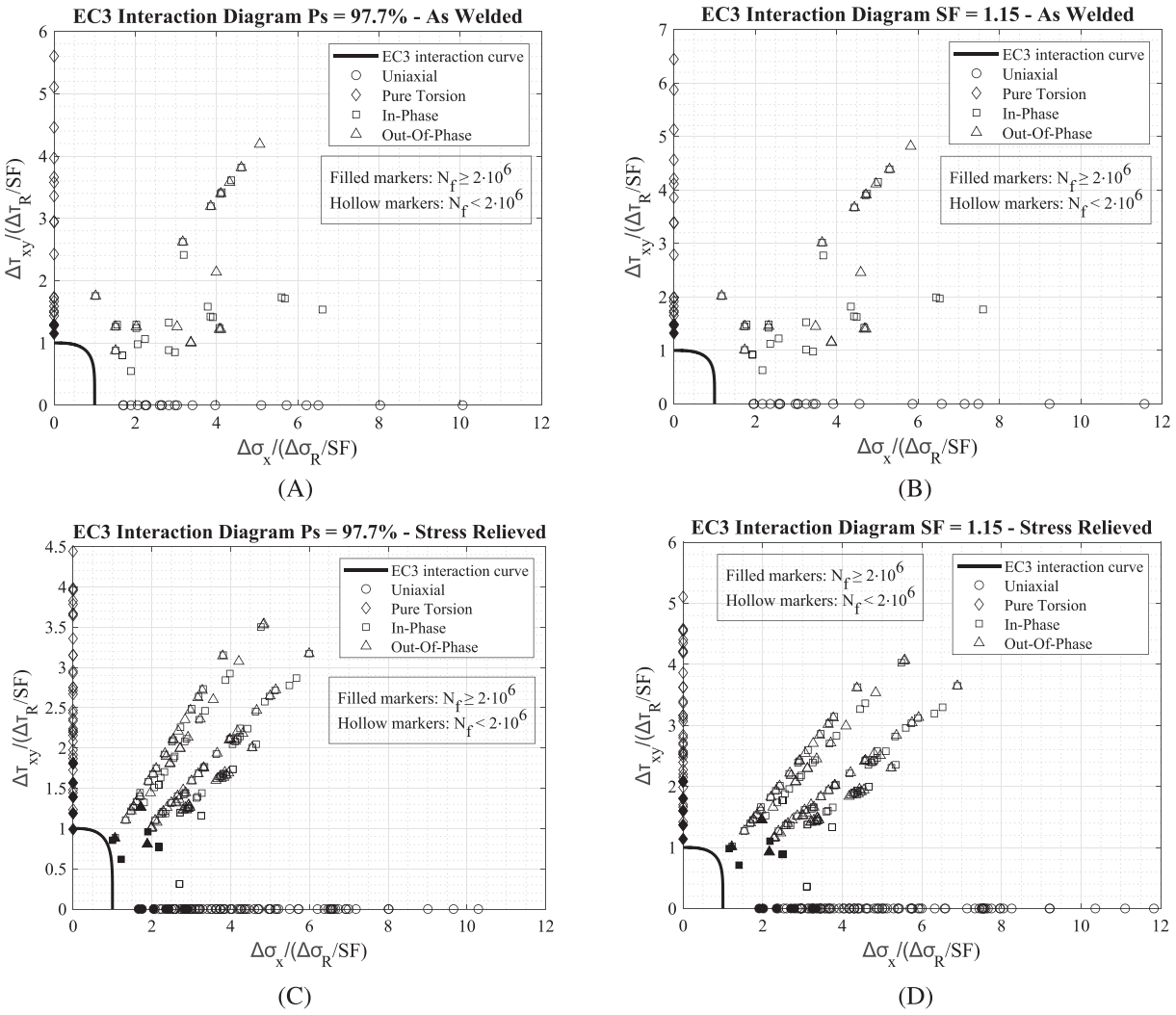

FIGURE 14 Hot spot stress (HSS) approach: EC3 interaction diagram for as-welded (A, B) and stress-relieved (C, D) steel welded joints under CA fatigue loading, with reference stresses ($\Delta\sigma_R$ and $\Delta\tau_R$) recalculated based on Ps = 97.7% and SF = 1.15.

interaction equation criterion with equivalent stress range substitution alongside the NS approach. Remarkably, no instances of non-conservative estimates were observed, indicating that the accuracy of the IIW approach in predicting the fatigue life of the steel welded joints under VA loading is satisfactory. When the IIW P-M is concerned, the fatigue life estimations shown in Figure 11c clustered within the uniaxial and torsional scatter bands and predominantly fell above the $N_f = N_{f,e}$ diagonal line. These findings demonstrate that the IIW P-M rule yielded conservative estimations for the fatigue life of the steel welded joints, ensuring a high level of safety.

Furthermore, when considering aluminum welded joints under VA loading, the IIW interaction equation criterion with equivalent stress range substitution also displayed the absence of non-conservative estimates. As depicted in Figure 12A,B, the fatigue life estimations in both cases were notably distant from the curve boundary defining the design safety level. Meanwhile, when applying the NS approach in conjunction with the IIW P-M rule as shown in Figure 12C and EC9 P-M rule as shown in Figure 12D for assessing aluminum welded joints under VA loading, the fatigue life estimations predominantly resided above the $N_f = N_{f,e}$ diagonal line. This observation highlights the conservative nature of the estimations, particularly when compared to the fatigue life estimations for steel welded joints resulting from the reanalysis.

5 | REANALYSES USING THE HOT SPOT STRESS (HSS) APPROACH

The HSS approach, also known as the structural or geometrical stress approach, is a highly effective

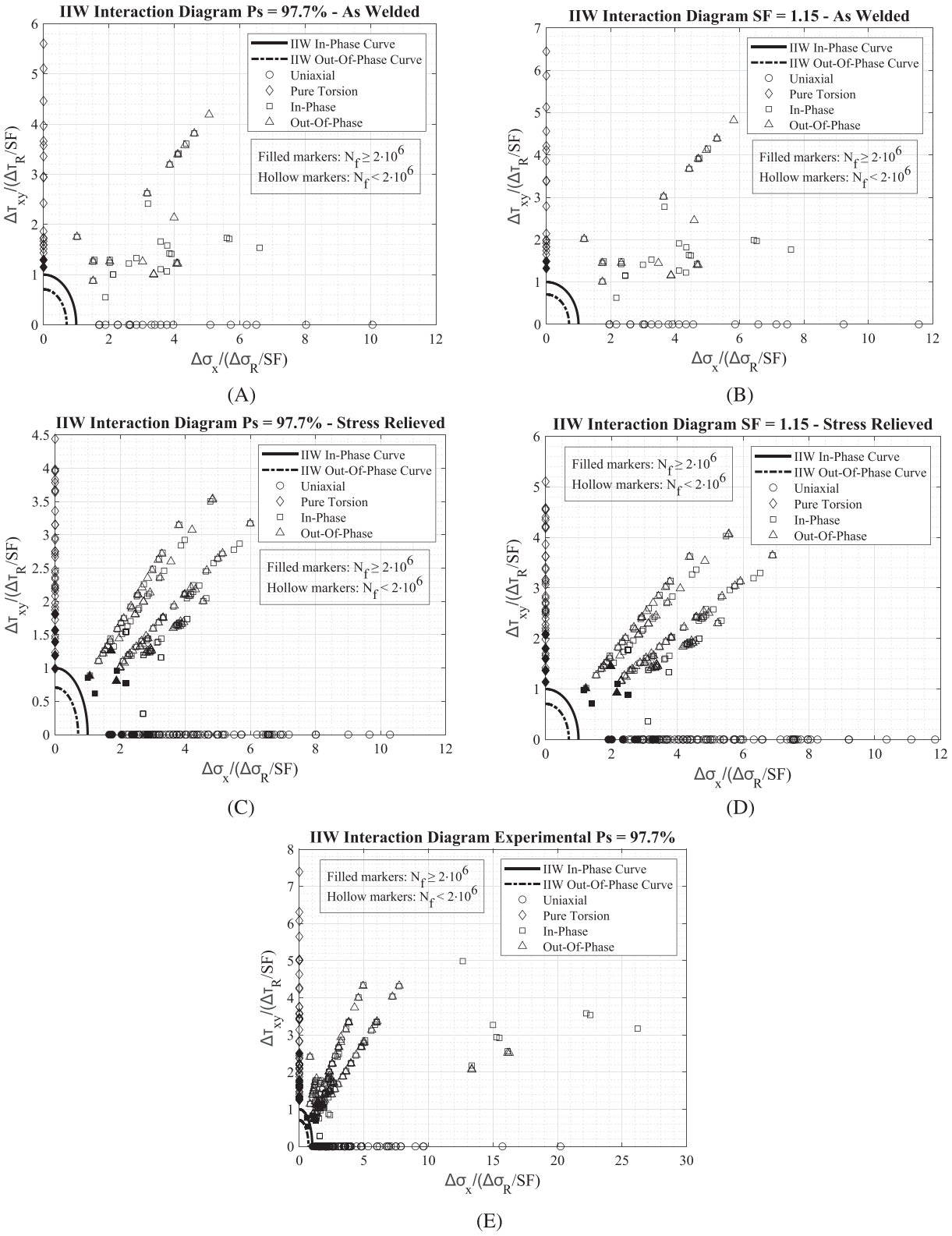

FIGURE 15 Hot spot stress (HSS) approach: IIW interaction diagram for as-welded (A, B) and stress-relieved (C, D) steel welded joints under CA fatigue loading, with reference stresses ($\Delta\sigma_R$ and $\Delta\tau_R$) recalculated based on $Ps = 97.7\%$, $SF = 1.15$, and experimental data.

methodology used for analyzing welded joints with intricate geometries, especially when deriving nominal stress poses challenges.[1–3,15,45,47] Unlike the conventional NS approach that only considers stresses from the nominal section of the joint, the HSS approach takes into account the stress concentration effects arising from the overall

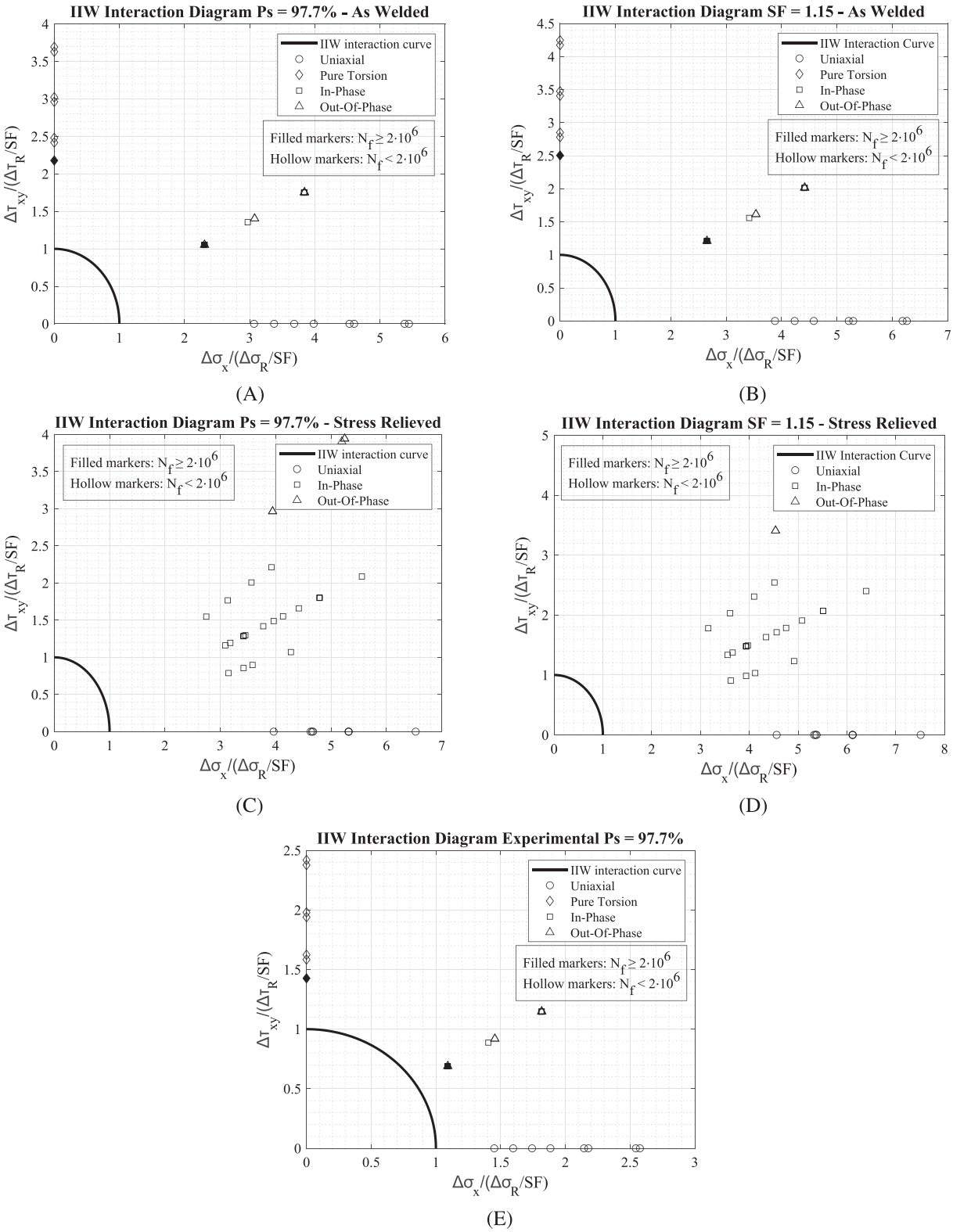

FIGURE 16 Hot spot stress (HSS) approach: IIW interaction diagram for as-welded (A, B) and stress-relieved (C, D) aluminum welded joints under CA fatigue loading, with reference stresses ($\Delta\sigma_R$ and $\Delta\tau_R$) recalculated based on $Ps = 97.7\%$, $SF = 1.15$, and experimental data.

structural intricacies while excluding stresses induced by the localized weld toe geometry as illustrated in Figure 3. Essentially, the HSS combines two distinct stresses: membrane stress and shell bending stress.[1,3,47,57]

Typically, the HSS approach can be determined through two methods: deriving stresses using FEA or utilizing strain measurements from strain gauges located at designated reference points near the weld toe.[1–3,15,45,47,57]

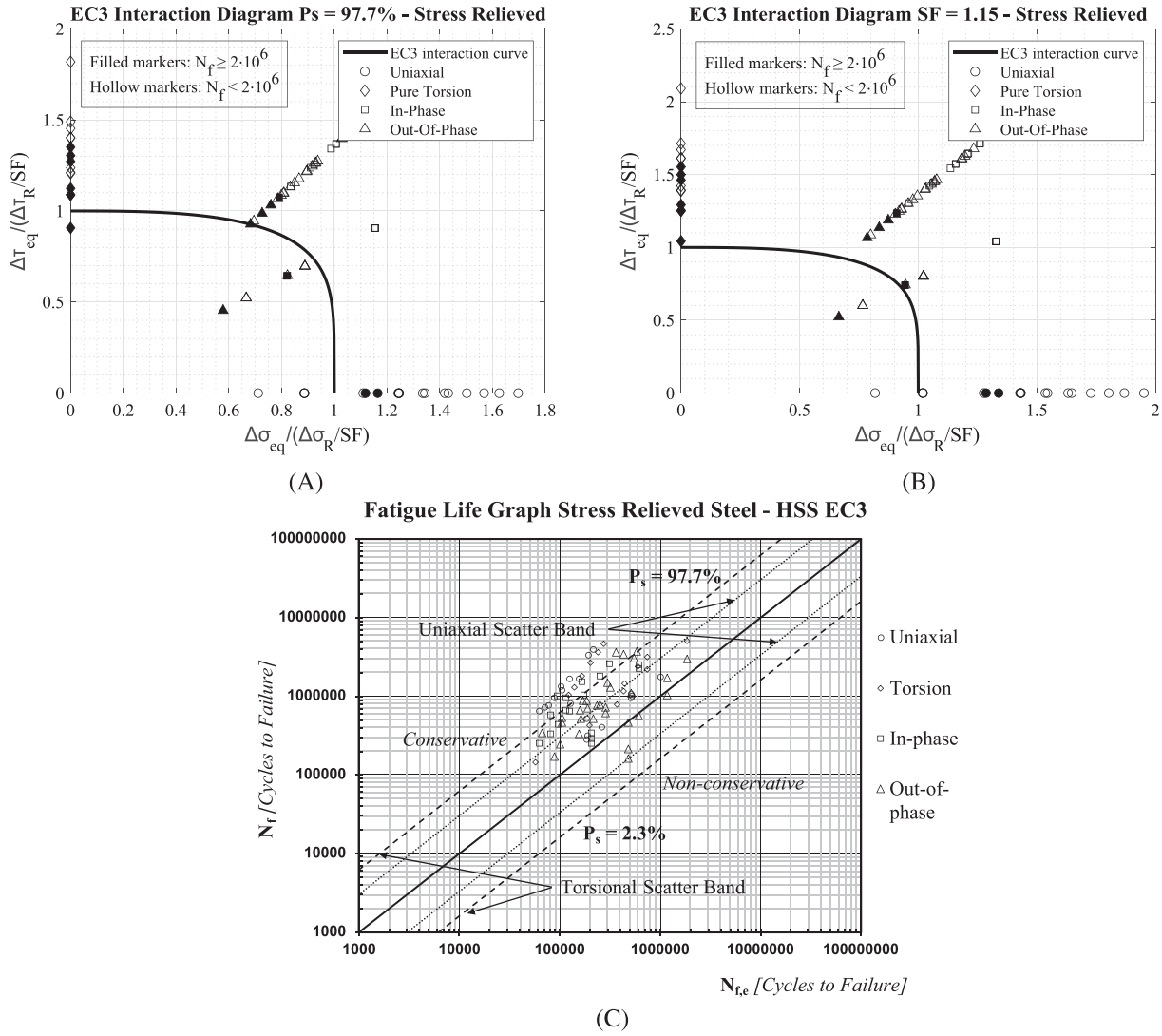

FIGURE 17 Hot spot stress (HSS) approach: EC3 interaction diagram (A, B) and fatigue life graph (C) for stress-relieved steel welded joints under VA fatigue loading, with reference stresses ($\Delta\sigma_R$ and $\Delta\tau_R$) recalculated based on $Ps = 97.7\%$ and $SF = 1.15$

However, for the purpose of this review, our attention will be exclusively directed towards the FEA-based approach for deriving the hot spot stress. This decision is based on the observation that the majority of the literature reviewed does not employ methods involving strain gauges, which rely heavily on experimental investigations.[18,27,36–43] By focusing on the FEA method, we can gain comprehensive insights into the hot spot stress analysis of welded joints in the context of the reviewed literature.

In the context of the HSS approach derived through FEA, both EC3 and the IIW propose a method of linearly extrapolating the hot spot stress from two designated reference points. To ensure precise and reliable results, it is crucial to employ fine meshes in the FE model. It is recommended to position these reference points at distances of 0.4t and 1.0t away from the weld toe, with "t" representing the reference plate thickness.[1,3,47,57] The rationale behind selecting these specific reference points is to ensure the exclusion of any notch stresses induced by the weld toe itself, thus enhancing the accuracy of the analysis.[1,3,15] The HSS extrapolation method is mathematically represented by Equation (11), showcasing the quantitative approach to deriving hot spot stress:

$$\sigma_{HSS} = 1.67\,\sigma_{0.4t} - 0.67\,\sigma_{1.0t} \tag{11}$$

Figure 13 provides a visual representation of the HSS derivation process using FEA with a fine mesh, offering clarity on the methodology employed.[1,3,47,57] To complement the information from Table 3, Table 4 presents key characteristics of the reanalyzed welded joints under CA loading using the HSS approach, focusing specifically on this method instead of the NS approach.

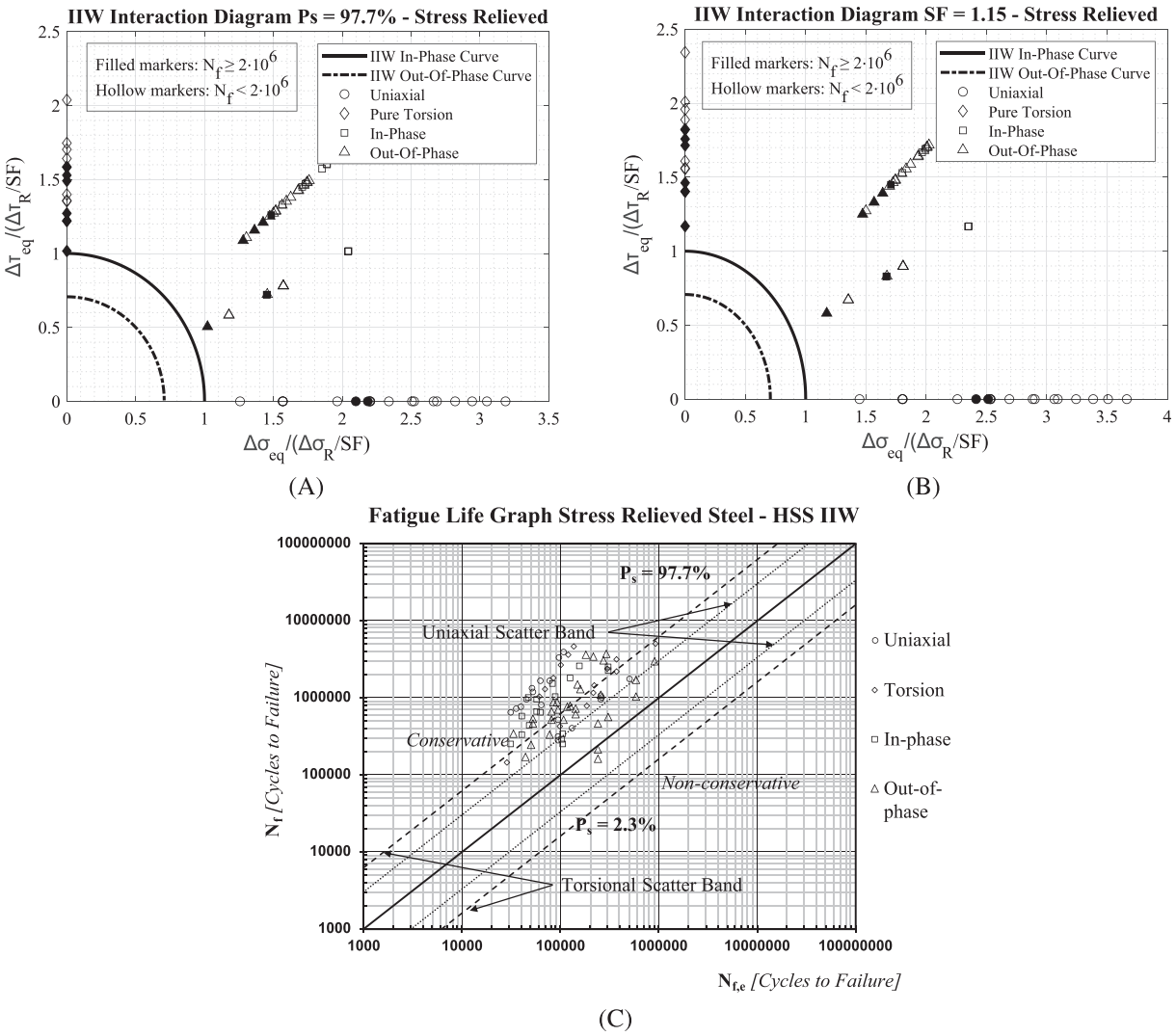

FIGURE 18 Hot spot stress (HSS) approach: IIW interaction diagram (A, B) and fatigue life graph (C) for stress-relieved steel welded joints under VA fatigue loading, with reference stresses ($\Delta\sigma_R$ and $\Delta\tau_R$) recalculated based on $Ps = 97.7\%$ and $SF = 1.15$.

The reanalysis results of the EC3 criterion under CA loading with the HSS approach are depicted in Figure 14 for both as-welded and stress-relieved steel welded joints. Notably, the recalculation of reference fatigue strength, considering $Ps = 97.7\%$ and an additional SF of 1.15, revealed no instances of non-conservative estimates.

Shifting our attention to the IIW criterion under CA loading and its implementation with the HSS approach, Figure 15 showcases the reanalysis graph specifically for steel welded joints, whereas Figure 16 presents the reanalysis graph for aluminum welded joints. For both as-welded and stress-relieved steel joints, the recalculation of reference stresses using $Ps = 97.7\%$, $SF = 1.15$, and experimental data yielded no non-conservative estimates. This further validates the effectiveness and accuracy of the HSS approach in assessing the fatigue behaviour of different welded joints. However, similar to the NS approach discussed earlier, it is essential to note that the HSS approach also demonstrates a significant degree of conservatism when applied to aluminum welded joints.

Table 4 also offers a summary focusing on welded joints investigated under VA loading using the HSS approach. Figure 17 illustrates the reanalysis of the EC3 criterion in conjunction with the HSS approach for stress-relieved steel welded joints under VA loading. The analysis revealed six instances of non-conservative estimates for the steel welded joints, corresponding to a P_{NC} of 7.41% using the EC3 interaction equation criterion with equivalent stress range substitution. Nevertheless, after applying an additional SF of 1.15, the number of non-conservative estimates reduced to 3 instances, resulting in a P_{NC} of 3.7%.

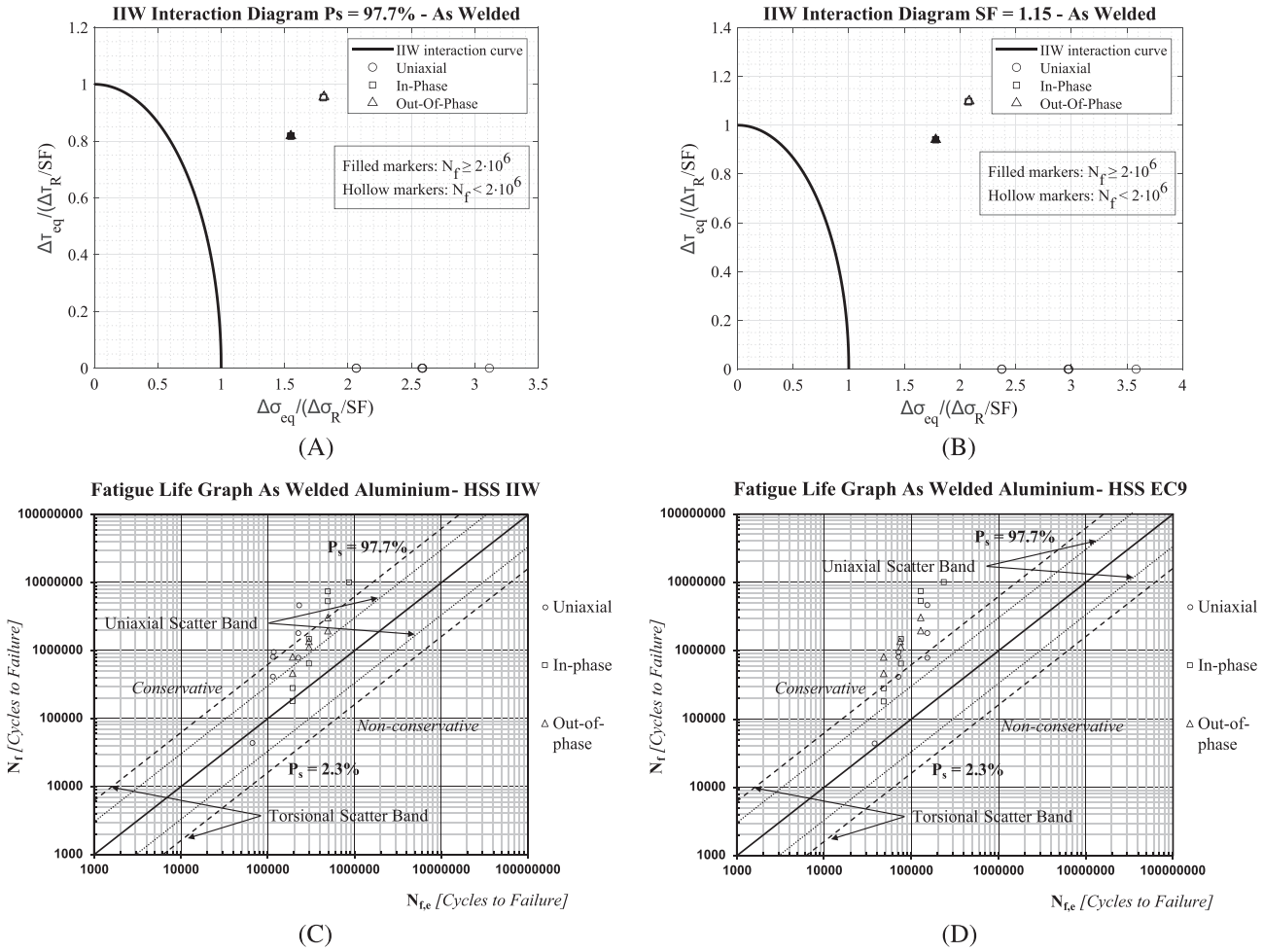

FIGURE 19 Hot spot stress (HSS) approach: IIW interaction diagram (A, B), IIW fatigue life graph (C), and EC9 fatigue life graph (D) for as-welded aluminum welded joints under VA fatigue loading, with reference stresses ($\Delta\sigma_R$ and $\Delta\tau_R$) recalculated based on $Ps = 97.7\%$ and $SF = 1.15$.

Furthermore, Figure 17C illustrates the reanalysis of stress-relieved steel welded joints using the EC3 P-M rule with the HSS approach for VA loading. The fatigue life estimations for these welded joints predominantly clustered within the uniaxial and torsional scatter band, with most of them falling above the $N_f = N_{f,e}$ diagonal line. This pattern demonstrates accurate and conservative estimations, highlighting the reliability of the EC3 interaction equation criterion with the HSS approach for VA loading.

Figure 18 presents the reanalysis results of steel welded joints using the IIW criteria with the HSS approach under VA loading.

In contrast to the EC3 interaction criterion, the IIW approach exhibits zero instances of non-conservative estimates for the steel welded joints. Moreover, when focusing on the IIW P-M rule, the fatigue life estimations for the steel welded joints mainly cluster within the uniaxial and torsional scatter band, and significantly, most of them fall above the $N_f = N_{f,e}$ diagonal line. This pattern highlights the accuracy and conservative nature of the estimations, as illustrated in Figure 18C.

Similarly, the reanalysis of aluminum welded joints under VA loading, as shown in Figure 19, reveals zero instances of non-conservative estimates, reaffirming the accuracy and dependability of the HSS approach in combination with the IIW interaction equation criterion. This finding underscores the reliability of the HSS approach for both steel and aluminum welded joints under VA multiaxial fatigue loading, providing accurate estimations for their fatigue life under different loading conditions.

Although the HSS approach offers the advantage of analyzing welded joints with intricate geometries, it does have certain limitations. One major limitation lies in its applicability only when fatigue failure originates from the weld toe region.[1–3,15,45,47,57] Furthermore, it is not suitable for situations where welded joints experience predominantly shear loading, as localized stress

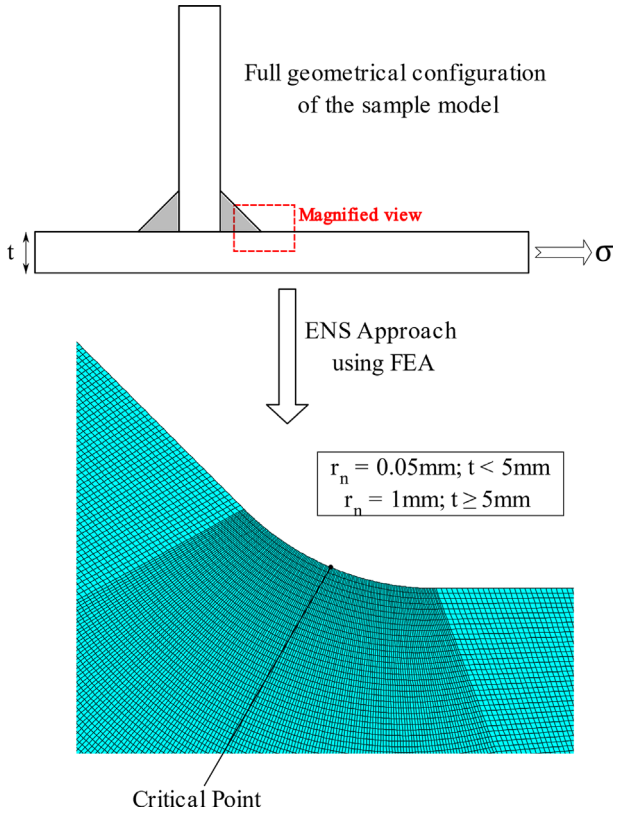

FIGURE 20 Application of effective notch stress (ENS) analysis approach on finely meshed finite element (FE) models. [Colour figure can be viewed at wileyonlinelibrary.com]

concentrations at notches were observed to occur at distances closer to the weld toe region than the recommended 0.4*t* reference point.[15,47] These limitations emphasize the importance of carefully considering and exploring alternative approaches when evaluating the fatigue behaviour of steel and aluminum welded joints.

6 | REANALYSES USING THE EFFECTIVE NOTCH STRESS (ENS) APPROACH

The ENS approach offers a unique and comprehensive methodology for evaluating welded joints. It incorporates the localized non-linear stress concentration effects arising from the weld toe or root geometry, as well as the overall structural characteristics.[3,11,15,44,45,47,49–51,57–59] This sets it apart from the NS and HSS approaches, which overlook these intricate factors. The IIW has put forth the ENS approach as a proposed method; however, it has yet to be included in the EC3.[1,3]

As per the guidelines provided by the IIW, effective notch stress can be obtained through the utilization of FEA. This involves introducing a fictitious notch at the weld toes and roots. For steel and aluminum welded joints with a plate thickness (*t*) equal to or exceeding 5 mm, the recommended fictitious notch radius is 1.0 mm. This recommendation, proposed by Hobbacher and embraced by the IIW, has been thoroughly validated and is extensively employed in practical applications involving welded joint thicknesses greater than 5 mm.[3,11,45,47,59–64]

However, for thin-walled welded joints with a thickness (*t*) below 5 mm, an alternative recommendation is needed to address the gap in the IIW's Hobbacher-based recommendation. To address this, Sonsino has put forth an alternative suggestion for the IIW ENS approach. Sonsino proposes a fictitious notch radius of 0.05 mm, specifically tailored for welded joint thicknesses less than 5 mm.[49,50,65] Furthermore, Sonsino recommends specific slope and reference fatigue strength (FAT value) values that are tailored to suit such "thin and flexible" welded joints.

Figure 20 visually demonstrates the practical application of the ENS approach using FEA to analyze both thin and thick-walled welded joints. In this comprehensive review, the recommendations put forth by both Hobbacher and Sonsino are incorporated, ensuring coverage across all levels of welded joint thickness within the IIW ENS approach.

Table 5 provides a concise summary of the reanalyzed welded joints under CA loading, offering valuable insights into their evaluation using the ENS approach. The table presents an overview of the uniaxial and torsional fatigue strengths (FAT values) recommended by the IIW standards. It also includes crucial details about the geometries of the welded joints, materials used, the slopes of the fatigue curves, and their respective sources of data.

To complement the tabular data, graphical representations in the form of Figures 21 and 22 visually depict the reanalysis results of steel and aluminum welded joints under CA loading, respectively, utilizing the IIW ENS approach. These figures offer a clear and concise depiction of the outcomes obtained from the analysis. It is important to note that the reference stresses for both as-welded and stress-relieved steel and aluminum joints have been recalculated, considering a $Ps = 97.7\%$ and an additional *SF* of 1.15. By applying these factors, the accuracy and reliability of the reanalyzed results are enhanced, ensuring a comprehensive evaluation of the welded joints.

The reanalysis results as shown in Figure 21 for steel welded joints under CA loading reveal an acceptable safety level for the assessment criteria with only two instances of non-conservative estimates at a $Ps = 97.7\%$ and decreases to zero non-conservative estimates when

TABLE 5 Summary of reanalyzed welded joints using ENS approach under CA and interaction equation criterion under VA fatigue loading, including uniaxial and torsional reference fatigue strengths, geometries, materials, fatigue curve slopes, and data sources.

Material	$\Delta\sigma_{R,\ Ps=97.7\%}$ [a] (MPa)	Uniaxial curve slope, k		$\Delta\tau_{R,\ Ps=97.7\%}$ [a] (MPa)	Torsional curve slope, $k0$		Geometry	Reference
		k (before knee point)[b]	k^* (after knee point)[b]		$k0$ (before knee point)[c]	$k0^*$ (after knee point)[c]		
(CA)	IIW	IIW	IIW	IIW	IIW	IIW		
UM StE 460[h]	225	3	22	160	5	22	Figure 4A	27
M StE 460[h]	225	3	22	160	5	22	Figure 4a	30
UM StE 460[h]	225	3	22	160	5	22	Figure 4E	30
StE 460[h]	225	3	22	160	5	22	Figure 4A	37
A519	225	3	22	160	5	22	Figure 4B	36
A519-A36[h]	225	3	22	160	5	22	Figure 4D	35
Fe 52 steel	225	3	22	160	5	22	Figure 4F	40
BS4360	630	3	22	250	5	22	Figure 4D	38
S340 + N, E355 + N	630	3	22	250	5	22	Figure 4E	41
S340 + N, E355 + N[h]	630	3	22	250	5	22	Figure 4E	41
St 35 ($t = 1$ mm)	630	3	22	250	5	22	Figure 4E	33
St 35 ($t = 2$ mm)	630	3	22	250	5	22	Figure 4E	31
6082-T6	71	3	22	63	5	22	Figure 4A	18
6060-T6[h]	180	3	22	90	5	22	Figure 4E	42
AW 6082	180	3	22	90	5	22	Figure 4E	33
AW 5042	180	3	22	90	5	22	Figure 4E	33
Material	$\Delta\sigma_{R,\ Ps=97.7\%}$ [a] (MPa)	Uniaxial curve slope, k		$\Delta\tau_{R,\ Ps=97.7\%}$ [a] (MPa)	Torsional curve slope, $k0$		Geometry	Reference
		k (before knee point)[b]	k' (before knee point)[b]		$k0$ (before knee point)[d]	$k0'$ (after knee point)[d]		
(VA)	IIW	IIW	IIW[(5)]	IIW	IIW	IIW[(5)]		
StE 460[h]	71	3	5	100	5	9	Figure 4A	34
StE 460[h]	71	3	5	100	5	9	Figure 4A	37
42CrMo4[h]	-	-	-	100	5	9	Figure 4E	28
6082-T6	32	3	5	36	5	9	Figure 4A	29

Abbreviations: M, machined; UM, unmachined.
[a]Reference normal and shear stresses extrapolated at 2 million cycles to failure, with a probability of survival (Ps) = 97.7%.
[b]The knee point for the IIW in terms of normal stress is located at the number of cycles to failure (N_{kp}) = 10^7 cycles.
[c]The knee point for the IIW in terms of shear stress is located at $N_{kp} = 10^8$ cycles.
[d]Slopes (k' and $k0'$) suggested by the IIW for VA loading are derived from Haibach's modification ($2k - 1$), where k is the slope before the knee point.
[e]Stress-relieved.

additional $SF = 1.15$ is applied. Again, when examining aluminum welded joints as shown in Figure 22, there were no instances of non-conservative estimates, highlighting a significant degree of conservatism in the analysis. All data points were noticeably distant from the curve boundary that establishes the design safety level.

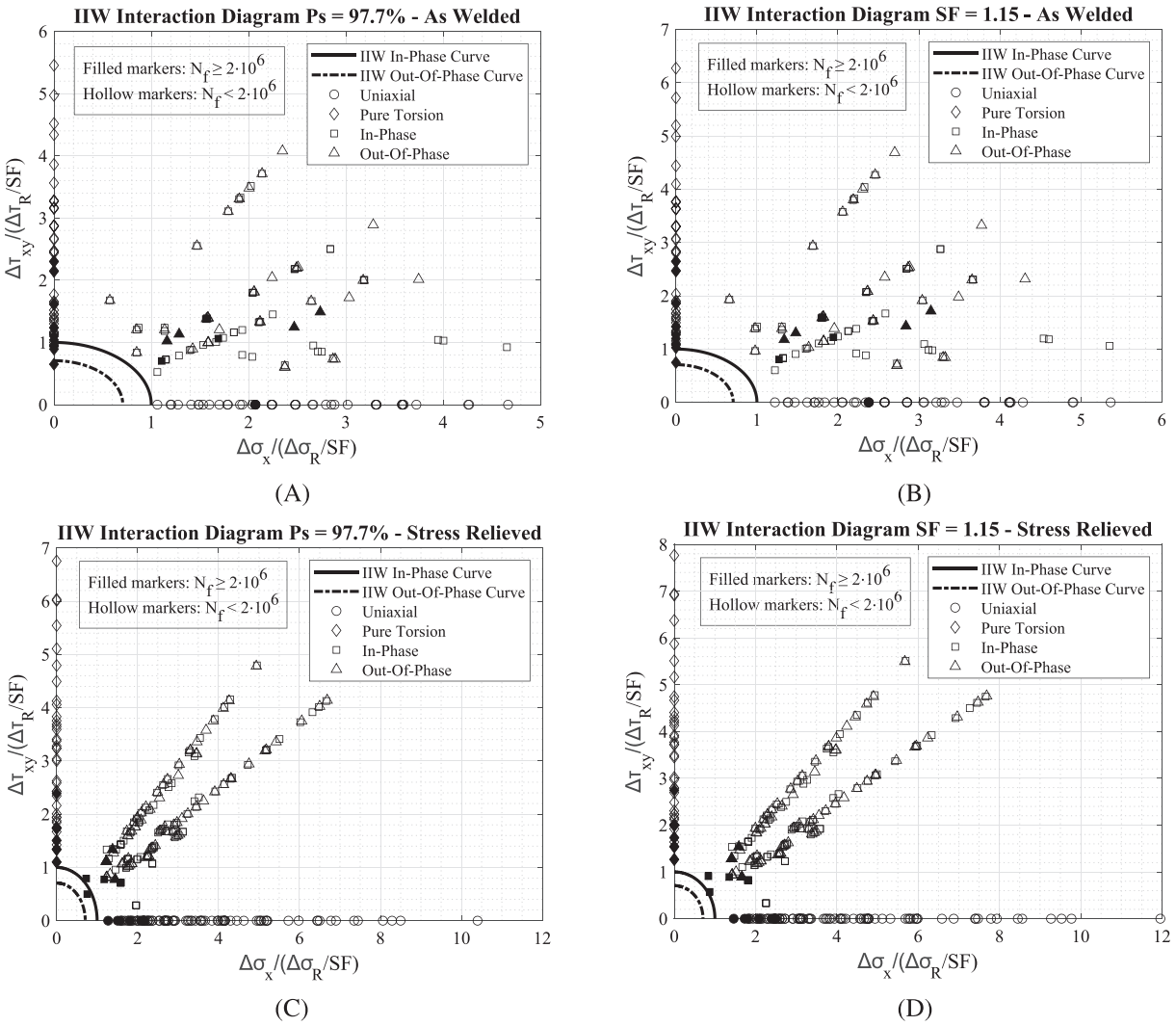

FIGURE 21 Effective notch stress (ENS) approach: IIW interaction diagram for as-welded (A, B) and stress-relieved (C, D) steel welded joints under CA fatigue loading, with reference stresses ($\Delta\sigma_R$ and $\Delta\tau_R$) recalculated based on $Ps = 97.7\%$ and $SF = 1.15$.

Table 5 also provides a concise summary of the reanalyzed welded joints under VA loading. In contrast to the observations obtained from CA fatigue loading, the ENS approach proved to be highly effective under VA fatigue loading, showing only one instance of non-conservative estimate with a P_{NC} of 1.23%. After applying the additional $SF = 1.15$, no non-conservative estimates were observed, reaffirming the accuracy and conservative nature of the estimations for steel welded joints as illustrated in Figure 23.

Similarly, when assessing aluminum welded joints under VA loading using the ENS approach, no instances of non-conservative estimates were identified as shown in Figure 24.

When utilizing the IIW P-M rule under VA loading in combination with the ENS approach, the fatigue life estimations for steel and aluminum welded joints predominantly clustered within the scatter band and positioned above the $N_f = N_{f,e}$ diagonal line as depicted in Figures 23c and 24c. These observations indicate accurate and conservative estimations for the fatigue life of both steel and aluminum welded joints under VA loading conditions.

Although the ENS approach surpasses the NS and HSS approaches in its ability to evaluate stress distribution within welded joints, it is important to acknowledge its limitations in practical scenarios. One notable constraint arises from the significant variations observed in the local profile of the weld toe along the weld line in real-world applications, resulting in discrepancies between physical welded joints and their FE model counterparts.[3,11,15,66] Additionally, the ENS approach mandates the use of a fine mesh to precisely capture the behaviour of the investigated welded joints. As a consequence, this requirement renders the process time-consuming and labour-intensive, especially when dealing

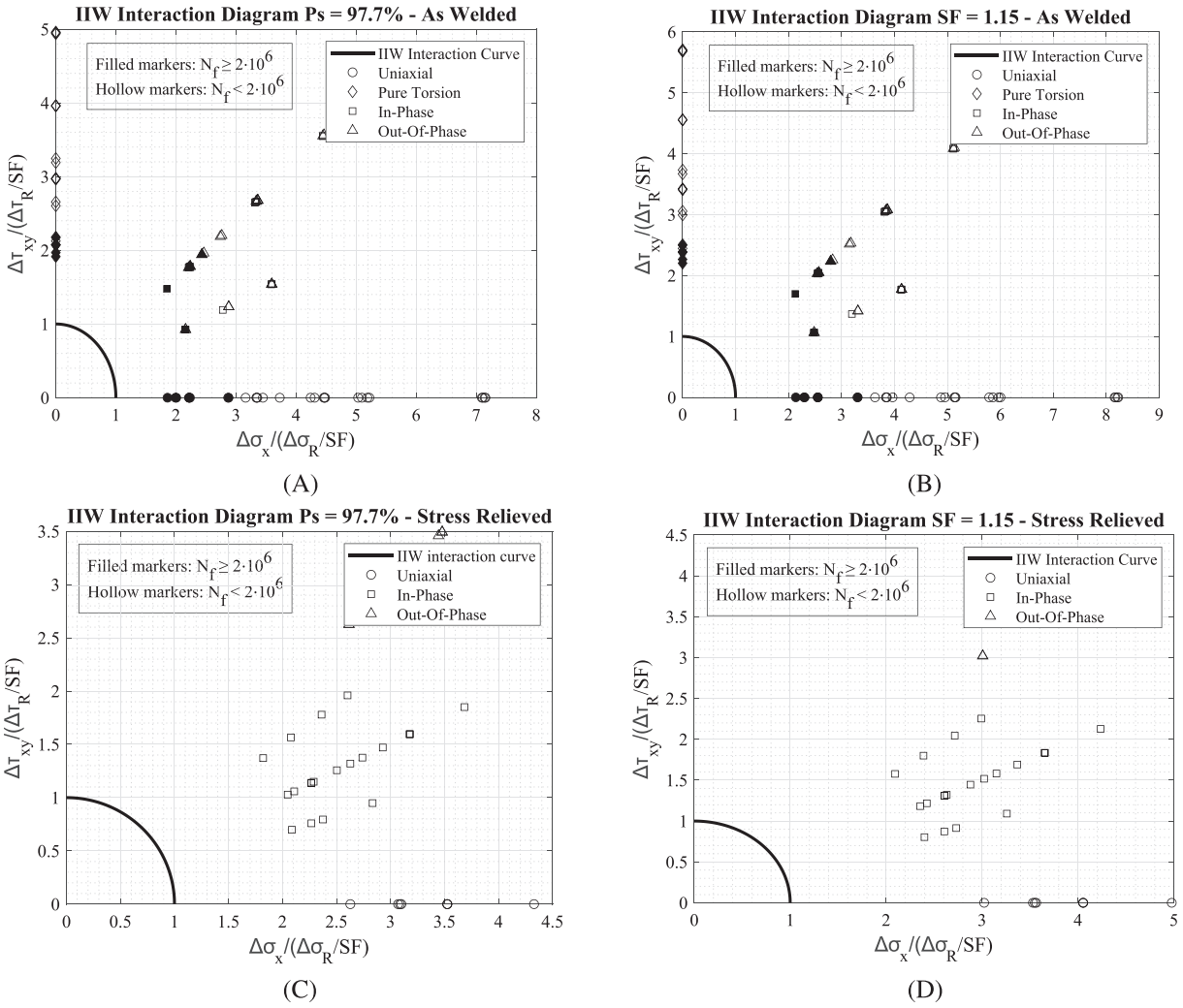

FIGURE 22 Effective notch stress (ENS) approach: IIW interaction diagram for as-welded (A, B) and stress-relieved (C, D) aluminum welded joints under CA fatigue loading, with reference stresses ($\Delta\sigma_R$ and $\Delta\tau_R$) recalculated based on $Ps = 97.7\%$ and $SF = 1.15$.

with intricate geometries frequently encountered in real engineering applications.[3,11,15,66]

7 | DISCUSSION

The assessment of welded joints and the assessment of conservatism in current standards offer significant insights into their behaviour. It is important to emphasize that the assessments regarding the level of conservatism in the reanalysis outcomes are established using design lines and FAT values with $Ps = 97.7\%$ and the additional SFs, specifically $SF = 1.15$ as recommended by both EC3 and the IIW, instead of relying on design lines and FAT values derived from Ps = 50%. An important observation revolves around the conservatism witnessed in estimations for aluminum welded joints, arising from the limited availability of testing data validating the reference fatigue strength.[18,32,33,42] Further experimental studies are imperative to refine the precision of assessments for these joints, ultimately ensuring more reliable evaluations.

It is crucial to emphasize that the determined level of safety is specifically applicable to the welded joints under examination. Therefore, it is vital not to extend this degree of conservatism to all loading applications. Nonetheless, this reanalysis stands as a crucial reference point, offering invaluable insights for engineering judgment. In instances involving critical welded joints, particularly in extensive structures like bridges and ships where conducting experimental tests is impractical, mandatory inspections take precedence in the evaluation process. The knowledge gained from these inspections plays a pivotal role in refining calculation procedures for similar loading scenarios in the future.

Additionally, a crucial consideration arises from the differentiation between the exponents in the EC3 and IIW interaction equations as shown in Equations (1)–(4).

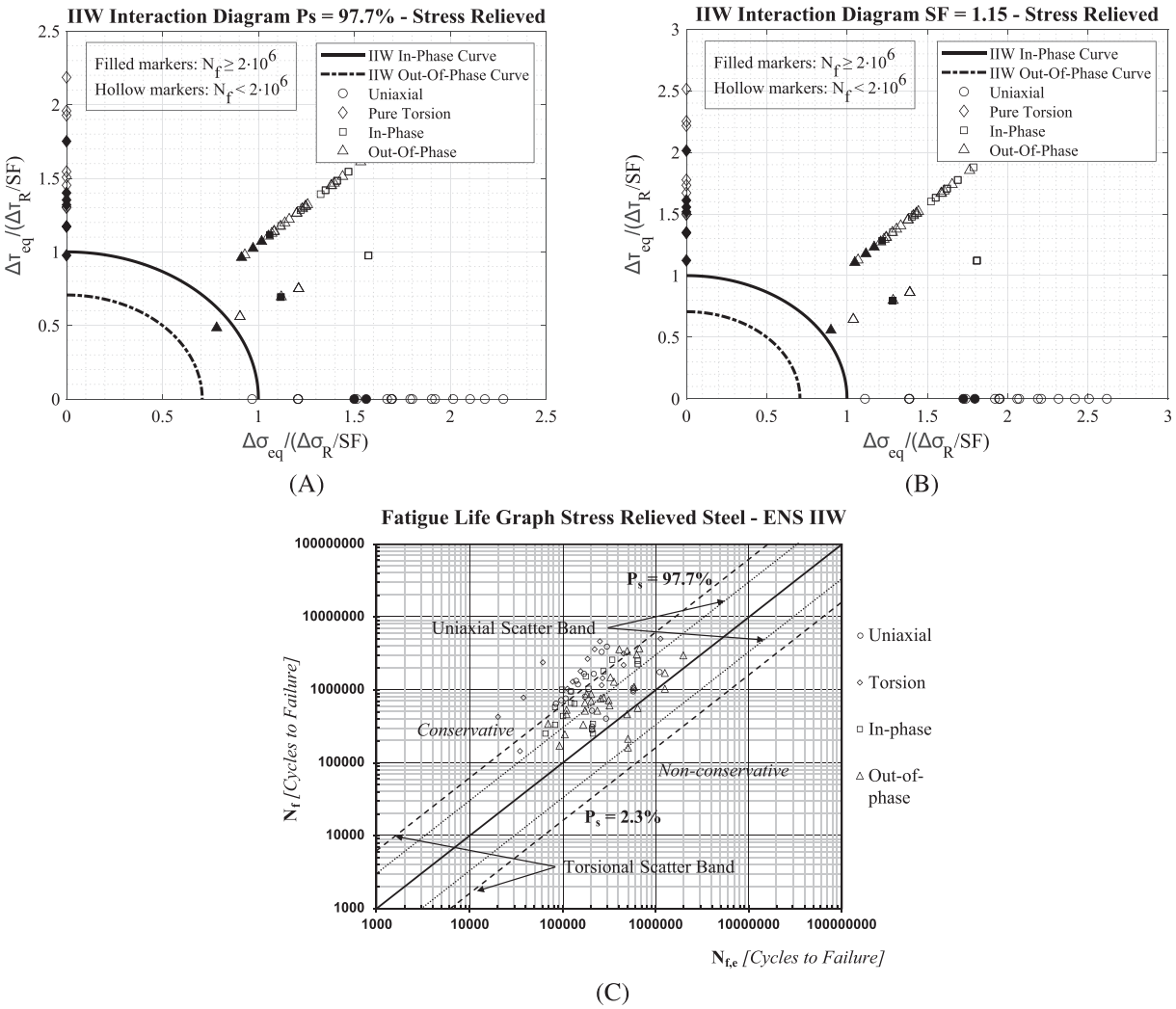

FIGURE 23 Effective notch stress (ENS) approach: IIW interaction diagram (A, B) and fatigue life graph (C) for stress-relieved steel welded joints under VA fatigue loading, with reference stresses ($\Delta\sigma_R$ and $\Delta\tau_R$) recalculated based on $Ps = 97.7\%$ and $SF = 1.15$

Although the 3 and 5 exponents in EC3 align closely with the slopes for uniaxial and pure torsional SN curves, there has been no scientific derivation of this equation presented.[1,54] Conversely, the exponents of 2 proposed by IIW are linked to the Gough–Pollard relationship, with 1 on the right-hand side of the equation derived from von Mises' criterion. The modification of 0.5 on the right-hand side of the equation serves as an engineering compromise to accommodate non-proportional loading scenarios to the best extent possible.[3,25,26,54,67] Nevertheless, it should not be assumed to universally cover all such scenarios. This highlights the intricacy of conducting experimental tests and inspections to ensure the safety of welding components.

Another significant observation concerns the slopes utilized for standard cases. According to EC3 and IIW recommendations, the suggested inverse slope for the uniaxial and torsional design S–N curve is 3 and 5, respectively.[1–3] Although these recommended values are appropriate for thick and rigid joints, thinner and more flexible joints exhibit shallower slopes when compared to the experimentally derived slopes recommended by EC3 and the IIW. This disparity significantly impacts the fatigue life estimation of a designed welded joint, particularly under VA loading Condition 7.[49] The consequence of a shallower predicted slope is a shorter fatigue life prediction at high stress levels and a longer fatigue life estimation at lower stress levels.[49] To address this issue, it would be useful to consider an inverse slope of 5 for the uniaxial curve and 7 for the torsional curve.[7,49]

A notable trend emerges in the fatigue life estimations for steel and aluminum welded joints under VA fatigue loading. The IIW P-M rule consistently exhibits greater conservatism compared to its EC counterpart. This difference may be attributed to the higher allowable damage sum factor for EC3 and EC9, as opposed to that of IIW. Nonetheless, it is crucial to highlight that both

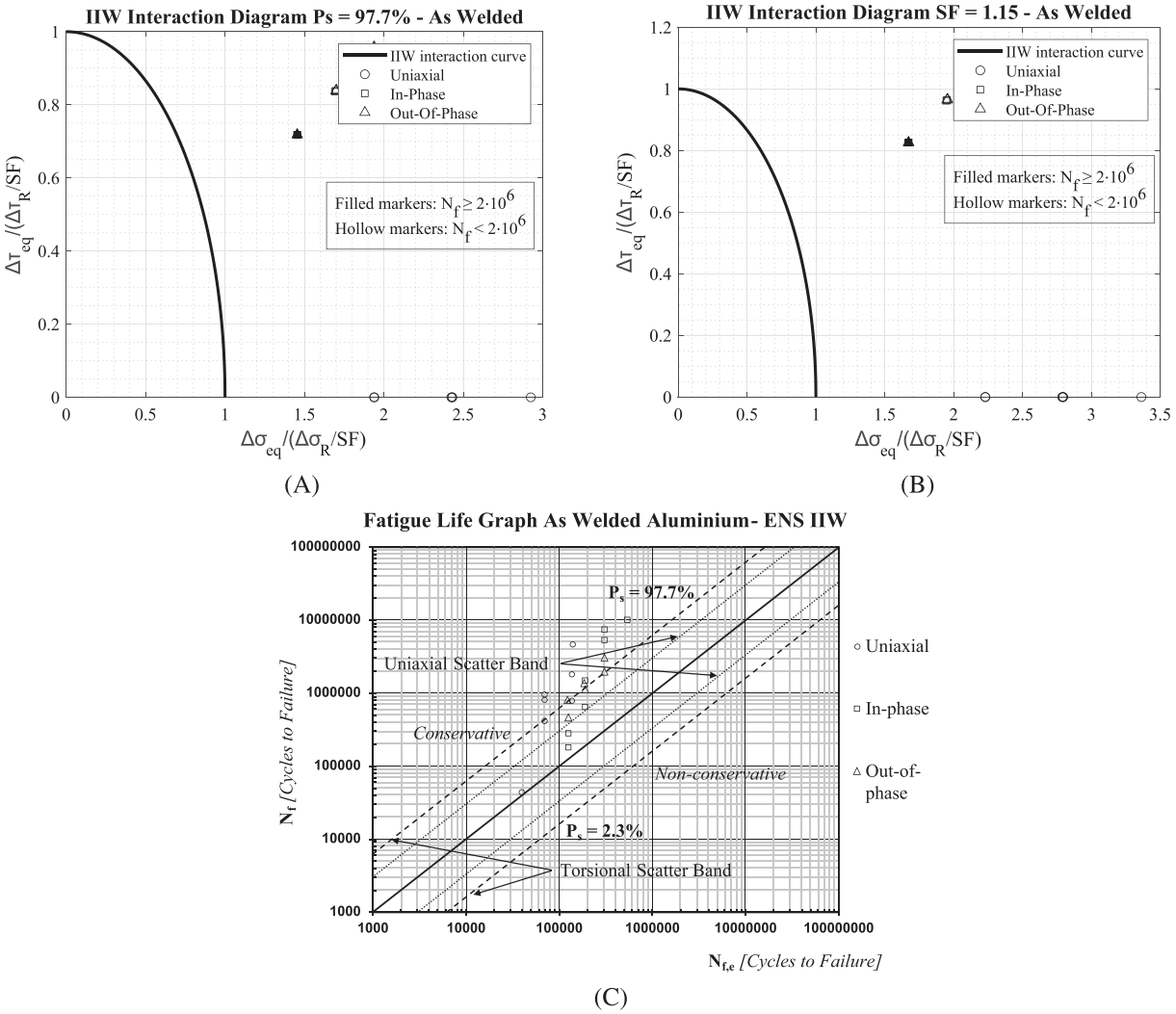

FIGURE 24 Effective notch stress (ENS) approach: IIW interaction diagram (A, B) and fatigue life graph (C) for as-welded aluminum welded joints under VA fatigue loading, with reference stresses ($\Delta\sigma_R$ and $\Delta\tau_R$) recalculated based on $Ps = 97.7\%$ and $SF = 1.15$.

estimations fall within the conservative range, ensuring safety.

Given the limited availability of fatigue data for steel and aluminum welded joints under VA multiaxial fatigue loading, there is a pressing need for future research to concentrate on this area. The objective is to validate the proposed fatigue assessment criteria, guaranteeing their precision and cost-effectiveness in the design of welded joints, a scenario commonly encountered in practical engineering applications.

In summary, both EC3 and the IIW consistently exhibit a commendable degree of conservatism. This remains consistent irrespective of the stress analysis methods employed, whether under CA or VA loading conditions. In particular, the HSS approach as per the IIW recommendation, proves to be the safest, with a consistent P_{NC} of 0%, irrespective of the loading conditions. However, it has limitations in cases where the critical point of the welded joint is at the weld root. In such instances, the IIW-ENS approach emerges as the next best option, accommodating all scenarios and ensuring safe estimations. These findings are supported by the comprehensive overview presented in Table 6a, b, which highlights the percentage of non-conservative estimates, P_{NC} derived from reanalyses of aluminum and steel welded joints. The dependability of these simpler multiaxial fatigue assessment methodologies, especially when compared to the more intricate critical plane approaches advocated by EC3 and the IIW, offers practitioners a solid basis for their design work.

8 | CONCLUSIONS

The comprehensive review of multiaxial fatigue assessment in steel and aluminum welded joints under CA and

TABLE 6 Summary of percentage of non-conservative estimates, P_{NC} from reanalyses of aluminum and steel welded joints under CA (a) and VA (b) fatigue loading using EC3 and IIW criteria with NS, HSS, and ENS approaches.

(a)

Percentage of non-conservative estimates, P_{NC} (%)												
Material	EC3-NS		IIW-NS			EC3-HSS		IIW-HSS			IIW-ENS	
	$Ps = 97.7\%$	$SF = 1.15$	$Ps = 97.7\%$	$SF = 1.15$	Exp[a]	$Ps = 97.7\%$	$SF = 1.15$	$Ps = 97.7\%$	$SF = 1.15$	Exp[a]	$Ps = 97.7\%$	$SF = 1.15$
Steel	2.54	0.85	1.27	0.42	0	0	0	0	0	0	1.02	0
Steel[b]	0.28	0	0	0	-	0	0	0	0	-	0.92	0
Aluminum	-	-	0	0	0	-	-	0	0	0	0	0
Aluminum[b]	-	-	0	0	-	-	-	0	0	-	0	0

(b)

Percentage of non-conservative estimates, P_{NC} (%)										
Material	EC3-NS		IIW-NS		EC3-HSS		IIW-HSS		IIW-ENS	
	$Ps = 97.7\%$	$SF = 1.15$	$Ps = 97.7\%$	$SF = 1.15$	$Ps = 97.7\%$	$SF = 1.15$	$Ps = 97.7\%$	$SF = 1.15$	$Ps = 97.7\%$	$SF = 1.15$
Steel[b]	11.1	3.70	0	0	7.41	3.70	0	0	1.23	0
Aluminum	-	-	0	0	-	-	0	0	0	0

[a]Exp denotes experimental data.
[b]Stress-relieved.

VA multiaxial fatigue loading using EC3 and IIW criteria in conjunction with NS, HSS, and ENS approaches reveals the key findings summarized in what follows:

- Both the IIW and EC3 criteria demonstrate a remarkable level of conservatism for steel welded joints, with a P_{NC} close to 0% irrespective of the stress analysis methods employed, especially under CA fatigue loading.
- The assessment of aluminum welded joints under CA and VA fatigue loading displays a significantly higher level of conservatism across all stress analysis approaches as compared to steel welded joints. This is attributed to the limited availability of data for aluminum joints.[18,29,32,33,42]
- The IIW-HSS approach appears to be the safest method, consistently delivering a P_{NC} of 0% across all loading conditions. However, limitations arise when the critical point of the welded joint is at the weld root. In such cases, the IIW-ENS approach proves to be the next best option, providing a solution that ensures safety in estimations across all scenarios.
- Based on the experimentally derived S–N curve slopes, the recommended inverse slopes for the uniaxial and torsional S–N curves should be revised from 3 and 5 to 5 and 7, respectively for both EC3 and the IIW recommendations to ensure accurate fatigue life estimations for thin and flexible welded joints.[49]
- The recommended exponents by EC3 criteria (3 for normal stress and 5 for shear stress) should undergo further verification and potential updates as the exponents of 2 suggested by the IIW demonstrate safer and more conservative estimations.[54]
- The stated level of conservatism is only applicable to the reanalyzed results and loading configuration presented in this quantitative review and, thus, cannot be extended and generalized to cater to all loading conditions as experimental testing under service loading conditions and inspections are mandatory during the evaluation process, especially when dealing with critical welded joints in extensive structures such as bridges, ships, or vessels.

DATA AVAILABILITY STATEMENT

The data that support the findings of this study are available from the corresponding author upon reasonable request.

NOMENCLATURE

$\Delta\sigma_x$	Normal stress range in the x direction
$\Delta\tau_{xy}$	Shear stress range in the xy direction
$\Delta\sigma_{eq}$	Equivalent normal stress range for VA loading
$\Delta\tau_{eq}$	Equivalent shear stress range for VA loading
$\Delta\sigma_R$	Reference normal stress extrapolated at 2 million cycles to failure
$\Delta\tau_R$	Reference shear stress extrapolated at 2 million cycles to failure
$\Delta\sigma_{NS}$	Effective normal stress range derived from nominal stress approach
$\Delta\sigma_{HSS}$	Effective normal stress range derived from hot spot stress approach
$\Delta\sigma_{ENS}$	Effective normal stress range derived from effective notch stress approach
$\Delta\tau_{NS}$	Effective shear stress range derived from nominal stress approach
$\Delta\tau_{HSS}$	Effective shear stress range derived from hot spot stress approach
$\Delta\tau_{ENS}$	Effective shear stress range derived from effective notch stress approach
D_{EC3}	Allowable damage sum for EC3 multiaxial fatigue assessment criteria under CA
D_{IIW}	Allowable damage sum for IIW multiaxial fatigue assessment criteria under CA
D_σ	Allowable damage sum due to normal stress
D_τ	Allowable damage sum due to shear stress
D_{tot}	Total allowable damage sum due to combined normal and shear stress damage
D_{crit}	Critical allowable damage sum under VA
CV	Comparison value for IIW interaction equation criterion under VA
$\Delta\sigma_{eff}$	Effective stress range
σ_{max}	Maximum stress value
σ_{min}	Minimum stress value
R	Load ratio
t	Welded joint plate thickness under loading
$\sigma_{0.4t}$	Stress state at $0.4t$ according to the hot spot stress linear extrapolation method
$\sigma_{1.0t}$	Stress state at $1.0t$ according to the hot spot stress linear extrapolation method
k	Negative inverse slope for the uniaxial fatigue S–N curve
$k0$	Negative inverse slope for the pure torsional fatigue S–N curve
k^*	Negative inverse slope for the uniaxial S–N curve after knee point under CA
$k0^*$	Negative inverse slope for the pure torsional S–N curve after knee point under CA
k'	Negative inverse slope for the uniaxial S–N curve after knee point under VA
$k0'$	Negative inverse slope for the pure torsional S–N curve after knee point under VA
D_{spec}	Specified Miner sum (allowable damage sum)
D_{al}	Allowable damage sum
D_{real}	Real damage sum derived experimentally
m_1	Slope above the knee point of the S–N curve

m_2	Slope below the knee point of the S–N curve
$\Delta\sigma_{i,S,d}$	Stress range above the knee point
$\Delta\sigma_{j,S,d}$	Stress range below the knee point
$\Delta\sigma_{L,d}$	Stress range at the knee point of SN curve
n_i	Number of cycles at applied stress range $\Delta\sigma_i$
n_j	Number of cycles at applied stress range $\Delta\sigma_j$
λ_i	Equivalent damage factor according to EC3 for VA
N_f	Experimental number of cycles to failure
$N_{f,e}$	Estimated number of cycles to failure
N_{kp}	Number of cycles at knee point (location of knee point)

ORCID

Chin Tze Ng https://orcid.org/0000-0002-0663-4798
Luca Susmel https://orcid.org/0000-0001-7753-9176

REFERENCES

1. Anon. Eurocode 3: design of steel structures—part 1–9: Fatigue. 2005.
2. Anon. Eurocode 9: design of aluminium structures—part 1–3: structures susceptible to fatigue. 2007.
3. Hobbacher A. *Recommendations for fatigue design of welded joints and components*. Vol. 47. Springer; 2016.
4. Sonsino CM, Baumgartner J, Breitenberger M. Equivalent stress concepts for transforming of variable amplitude into constant amplitude loading and consequences for design and durability approval. *Int J Fatigue*. 2022;162:106949.
5. Haibach E. *Modified linear damage accumulation hypothesis accounting for a decreasing fatigue strength during increasing fatigue damage*. Darmstadt Lab für Betriebsfestigkeit, LBF; 1970.
6. Susmel L. The modified Wöhler curve method calibrated by using standard fatigue curves and applied in conjunction with the theory of critical distances to estimate fatigue lifetime of aluminium weldments. *Int J Fatigue*. 2009;31(1):197-212.
7. Susmel L, Askes H. Modified Wöhler curve method and multiaxial fatigue assessment of thin welded joints. *Int J Fatigue*. 2012;43:30-42.
8. Susmel L. Three different ways of using the modified Wöhler curve method to perform the multiaxial fatigue assessment of steel and aluminium welded joints. *Eng Fail Anal*. 2009;16(4):1074-1089.
9. Susmel L. A simple and efficient numerical algorithm to determine the orientation of the critical plane in multiaxial fatigue problems. *Int J Fatigue*. 2010;32(11):1875-1883.
10. Susmel L, Tovo R, Benasciutti D. A novel engineering method based on the critical plane concept to estimate the lifetime of weldments subjected to variable amplitude multiaxial fatigue loading. *Fatigue Fract Eng Mater Struct*. 2009;32(5):441-459.
11. Pedersen MM. Multiaxial fatigue assessment of welded joints using the notch stress approach. *Int J Fatigue*. 2016;83:269-279.
12. Findley WN. A theory for the effect of mean stress on fatigue of metals under combined torsion and axial load or bending. *J Eng Ind*. 1959;81(4):301-305.
13. Susmel L, Tovo R. On the use of nominal stresses to predict the fatigue strength of welded joints under biaxial cyclic loading. *Fatigue Fract Eng Mater Struct*. 2004;27(11):1005-1024.
14. Mei J, Dong P. An equivalent stress parameter for multi-axial fatigue evaluation of welded components including non-proportional loading effects. *Int J Fatigue*. 2017;101:297-311.
15. Mei J, Dong P, Xing S, et al. An overview and comparative assessment of approaches to multi-axial fatigue of welded components in codes and standards. *Int J Fatigue*. 2021;146:106144.
16. Bäckström M, Marquis G. A review of multiaxial fatigue of weldments: experimental results, design code and critical plane approaches. *Fatigue Fract Eng Mater Struct*. 2001;24(5):279-291.
17. Papadopoulos IV. Critical plane approaches in high-cycle fatigue: on the definition of the amplitude and mean value of the shear stress acting on the critical plane. *Fatigue Fract Eng Mater Struct*. 1998;21(3):269-285.
18. Kueppers M, Sonsino CM. Critical plane approach for the assessment of the fatigue behaviour of welded aluminium under multiaxial loading. *Fatigue Fract Eng Mater Struct*. 2003;26(6):507-513.
19. Bruun ØA, Härkegård G. A comparative study of design code criteria for prediction of the fatigue limit under in-phase and out-of-phase tension–torsion cycles. *Int J Fatigue*. 2015;73:1-16.
20. Marquis G, Bäckström M, Siljander A. Multiaxial fatigue damage parameters for welded joints: design code and critical plane approaches. In: *1st North European Engineering and Science Conference (NESCO I)*. Engineering Materials Advisory Services EMAS; 1997.
21. Susmel L. *Multiaxial notch fatigue*. Vol. 81. Elsevier; 2009.
22. Susmel L. Four stress analysis strategies to use the modified Wöhler curve method to perform the fatigue assessment of weldments subjected to constant and variable amplitude multiaxial fatigue loading. *Int J Fatigue*. 2014;67:38-54.
23. Sonsino CM. Fatigue testing under variable amplitude loading. *Int J Fatigue*. 2007;29(6):1080-1089.
24. Eulitz K-G. Damage accumulation limitations and perspectives for fatigue life assessment. In: *Proceedings of Materials Week 2000*. 2000:25-28.
25. Sonsino CM, Maddox SJ, Hobbacher A. Fatigue life assessment of welded joints under variable amplitude loading-State of present knowledge and recommendations for fatigue design regulations. 2005.
26. Sonsino CM, Fricke W. Some remarks for improving the assessment of multiaxial stress states and multiaxial spectrum loading in the IIW-fatigue design recommendations. *IIW-Document No XIII-2158r1–07/XV-1250r1–07XIII-2128-06/XV-1222-06*. 2006: 4–19.
27. Sonsino CM. Multiaxial fatigue of welded joints under in-phase and out-of-phase local strains and stresses. *Int J Fatigue*. 1995;17(1):55-70.
28. Pyttel B, Grawenhof P, Berger C. Application of different concepts for fatigue design of welded joints in rotating components in mechanical engineering. *Int J Fatigue*. 2012;34(1):35-46.
29. Kueppers M, Sonsino CM. Assessment of the fatigue behaviour of welded aluminium joints under multiaxial spectrum loading by a critical plane approach. *Int J Fatigue*. 2006;28(5-6):540-546.
30. Sonsino CM. Fatigue behaviour of welded components under complex elasto-plastic multiaxial deformations. ECSC-Report No EUR 16024. 1997.
31. Sonsino CM, Kueppers M, Eibl M, Zhang G. Fatigue strength of laser beam welded thin steel structures under multiaxial loading. *Int J Fatigue*. 2006;28(5-6):657-662.

32. Wiebesiek J, Sonsino CM. New results in multiaxial fatigue of welded aluminium joints. *IIW-Document No XIII-2314-10/XV-1349-10*. 2010;13: 2310-2314.
33. Wiebesiek J, Störzel K, Bruder T, Kaufmann H. Multiaxial fatigue behaviour of laserbeam-welded thin steel and aluminium sheets under proportional and non-proportional combined loading. *Int J Fatigue*. 2011;33(8):992-1005.
34. Sonsino CM, Kueppers M. Multiaxial fatigue of welded joints under constant and variable amplitude loadings. *Fatigue Fract Eng Mater Struct*. 2001;24(5):309-327.
35. Siljander A, Kurath P, Lawrence FV Jr. *Proportional and non-proportional multiaxial fatigue of tube to plate weldments*. Univ Illinois Urbana-Champaign; 1989.
36. Yung J-Y, Lawrence FV Jr. Predicting the fatigue life of welds under combined bending and torsion. *Mech Eng Publ Biaxial Multiaxial Fatigue*. 1989;53-69.
37. Yousefi F, Witt M, Zenner H. Fatigue strength of welded joints under multiaxial loading: experiments and calculations. *Fatigue Fract Eng Mater Struct*. 2001;24(5):339-355.
38. Archer R. Fatigue of a welded steel attachment under combined direct stress and shear stress. In: *International Conference of Fatigue of Welded Constructions, No. Paper*. Vol 50. 1987.
39. Amstutz H, Störzel K, Seeger T. Fatigue crack growth of a welded tube–flange connection under bending and torsional loading. *Fatigue Fract Eng Mater Struct*. 2001;24(5):357-368.
40. Bäckström M, (Otamedia). *Multiaxial fatigue life assessment of welds based on nominal and hot spot stresses*. Technical Research Centre of Finland; 2003.
41. Shams E, Vormwald M. Fatigue of weld ends under combined loading. *Int J Fatigue*. 2017;100:627-638.
42. Costa JDM, Abreu LMP, Pinho ACM, Ferreira JAM. Fatigue behaviour of tubular AlMgSi welded specimens subjected to bending–torsion loading. *Fatigue Fract Eng Mater Struct*. 2005;28(4):399-407.
43. Razmjoo GR. Fatigue of load-carrying fillet welded joints under multiaxial loading. In: *5 Th International Conference on Biaxial/Multiaxial Fatigue & Fracture*. 1997:53-70.
44. Al Zamzami I, Susmel L. On the use of hot-spot stresses, effective notch stresses and the point method to estimate lifetime of inclined welds subjected to uniaxial fatigue loading. *Int J Fatigue*. 2018;117:432-449.
45. Radaj D. Review of fatigue strength assessment of nonwelded and welded structures based on local parameters. *Int J Fatigue*. 1996;18(3):153-170.
46. Van Lieshout PS, Den Besten JH, Kaminski ML. Comparative study of multiaxial fatigue methods applied to welded joints in marine structures. *Frat Ed Integrità Strutt*. 2016;10(37):173-192.
47. Niemi E. *Stress determination for fatigue analysis of welded components*. Woodhead Publishing; 1995.
48. Tovo R, Lazzarin P. Relationships between local and structural stress in the evaluation of the weld toe stress distribution. *Int J Fatigue*. 1999;21(10):1063-1078.
49. Sonsino CM, Bruder T, Baumgartner J. SN lines for welded thin joints—suggested slopes and FAT values for applying the notch stress concept with various reference radii. *Weld World*. 2010;54(11-12):R375-R392.
50. Sonsino CM, Fricke W, De Bruyne F, Hoppe A, Ahmadi A, Zhang G. Notch stress concepts for the fatigue assessment of welded joints–background and applications. *Int J Fatigue*. 2012;34(1):2-16.
51. Fricke W. IIW guideline for the assessment of weld root fatigue. *Weld World*. 2013;57(6):753-791.
52. Sines G. Behavior of metals under complex static and alternating stresses. *Met Fatigue*. 1959;1:145-169.
53. Atzori B. TRATTAMENTO TERMICI E RESISTENZA A FATICA DELLE STRUTTURE SOLDATE. 1983.
54. Sonsino CM, Wallmichrath M, Kueppers M. Assessment of multiaxial fatigue test results on welded joints by application of the IIW—formula and modifications. *IIW-Document No XIII-2046-05*. 2005.
55. Haibach E. Verfahren und Daten zur Bauteilberechnung. 1989.
56. Anon. Eurocode 1: Actions on structures—Part 3: Actions induced by cranes and machinery. 2006.
57. Radaj D, Sonsino CM, Fricke W. *Fatigue assessment of welded joints by local approaches*. Woodhead Publishing; 2006.
58. Susmel L, Sonsino CM, Tovo R. Accuracy of the modified wöhler curve method applied along with the rref = 1 mm concept in estimating lifetime of welded joints subjected to multiaxial fatigue loading. *Int J Fatigue*. 2011;33(8):1075-1091.
59. Schijve J. Fatigue predictions of welded joints and the effective notch stress concept. *Int J Fatigue*. 2012;45:31-38.
60. Radaj D, Lazzarin P, Berto F. Generalised Neuber concept of fictitious notch rounding. *Int J Fatigue*. 2013;51:105-115.
61. Morgenstern C, Sonsino CM, Hobbacher A, Sorbo F. Fatigue design of aluminium welded joints by the local stress concept with the fictitious notch radius of $r_f = 1$ mm. *Int J Fatigue*. 2006;28(8):881-890.
62. Fricke W. Round-robin study on stress analysis for the effective notch stress approach. *Weld World*. 2007;51(3-4):68-79.
63. Berto F, Lazzarin P, Radaj D. Fictitious notch rounding concept applied to V-notches with root hole subjected to in-plane mixed mode loading. *Eng Fract Mech*. 2014;128:171-188.
64. Atzori B, Lazzarin P, Meneghetti G, Ricotta M. Fatigue design of complex welded structures. *Int J Fatigue*. 2009;31(1):59-69.
65. Sonsino CM. A consideration of allowable equivalent stresses for fatigue design of welded joints according to the notch stress concept with the reference radii $r_{ref} = 1.00$ and 0.05 mm. *Weld World*. 2009;53(3-4):R64-R75.
66. Shen W, Yan R, He F, Wang S. Multiaxial fatigue analysis of complex welded joints in notch stress approach. *Eng Fract Mech*. 2018;204:344-360.
67. Sonsino CM, Wiebesiek J. Assessment of multiaxial spectrum loading of welded steel and aluminium joints by modified equivalent stress and Gough–Pollard algorithms. IIW-Document No XIII-2158r1-07/XV-1250r1–07. 2007.

How to cite this article: Ng CT, Sonsino CM, Susmel L. Multiaxial fatigue assessment of welded joints: A review of Eurocode 3 and International Institute of Welding criteria with different stress analysis approaches. *Fatigue Fract Eng Mater Struct*. 2024;1-34. doi:10.1111/ffe.14319